ROLE OF SURFACE CHEMISTRY IN MODIFYING THE OPTICAL PROPERTIES OF SILICON NANOSTRUCTURE

By
TSEGAYE BELEGE

SUBMITTED IN PARTIAL FULFILLMENT OF THE
REQUIREMENTS FOR THE DEGREE OF
MASTER OF SCIENCE IN MATERIALS SCIENCE
AT
ADDIS ABABA UNIVERSITY
ADDIS ABABA, ETHIOPIA

JUNE 2010

ADDIS ABABA UNIVERSITY
GRADUATE STUDIES

ROLE OF SURFACE CHEMISTRY IN MODIFYING THE OPTICAL PROPERTIES OF SILICON NANOSTRUCTURE

BY: **TSEGAYE BELEGE ATISME**

Materials Science Program
Faculty of Science

Approved by the Examining Board

Supervisor: _____

Dr. S. K Ghoshal

Examiners: _____

Prof. Teketel Yohannes

_____

Dr.Mesfin Redi

Acknowledgements

Above all, I would like to thank the almighty God for his endless charity. I am grateful to my advisor, Dr. S. K. Ghoshal for his critical and constructive suggestion, well planned follow up and constant support during this research, he was tireless, programmed, and ready to encourage me at any time when I consult him not only in my thesis work but also in my entire graduate study. As an advisor he put a lot of impression on me that I never forget whenever and wherever in my academic life; I want to forward my gratitude to professor Teketel Yohhanes for his unreserved academic and technical support.

I am indebted to express my heart felt gratitude to,my father Belege Atisme, Taye W/Aregay, Workezeb Belege, Habtamu Belege, Mennon Belege , Abrham Belege for their unlimited love and support.

I want to express my due appreciation to Addis Ababa University, Materials Science program, for providing this chance, rendering good office service during my stay, and I want to extend my acknowledgement to staff members of the program who devote their time for academic matters. Specially W/o Belaynesh who provide all the necessary materials during the course time.

Next with no words for me to express my heart feeling for her patience, I would like to thank Miss. Frehiwot Tekle for her great cooperation on conducting many of my affairs directly or indirectly on my life. Finally I would like to acknowledge Ministry of education for providing me sponsorship.

Table of content

Chapter Six

List of tables

List of figures

Abstract

We combine two model used earlier. We vary the fitting parameters C and α (which depend on surface, geometry, confinement, size, porosity and materials properties). We use surface energy (E_s = 0.05eV), binding energy (E_b = 0.07eV), C, and α using these as input we generate Eg and PL intensity spectra. The Eg and PL spectrum are compared with TB and PP data. The position of PL peak is used to find the band gap and compared with the experiment. The main objective is to use the already existing model, combining them and use fitting parameters to calculate optical properties like PL intensity and band gap for varying size. The results show qualitative agreement with the experiment. This is due to the simplicity of the model. However, we found it is interesting to use the fitting parameters C and α to show that our model is in good agreement with the experimental observation.

Declaration

This thesis is my original work, has not been presented for a degree in any other University and that all the sources of material used for the thesis have been dully acknowledged.

Name: Tsegaye Belege

Signature: _____

Place and time of submission: **Addis Ababa University, June 2010**

This thesis has been submitted for examination with my approval as University advisor.

Name: Dr. S. K Ghoshal

Signature: _____

Chapter One

Introduction

In this chapter we are going to see what silicon nanocrystallites are, their application in the real world, some of their fabrication methods and how the optical properties of nanostructure get affected by quantum confinement and surface passivation.

1.1 What are silicon nanocrystallites?

A nanocrystal is a crystalline material with dimensions measured in nanometers and a nanoparticle with a structure that is mostly crystalline in the interior. These materials are of huge technological interest since many of their optical, electronic and thermodynamic properties show strong size and surface dependence, and can therefore be controlled through careful manufacturing processes.

Silicon is the material of choice in microelectronic industries. This remarkable success is due to various factors such as the wide availability of silicon and the ease of producing the natural silicon from silicon oxide (SiO_2). It is the second most abundant element in the earth's crust next to oxygen. It constitutes about 28% by mass of the earth's crust.

One of the strategic objective of the nanotechnology concept is the development of new materials having nanometer size which have entirely new physical properties and, therefore, new functionality. Historically, nanostructured silicon was first produced by Ingeborg and Arthur Uhlir at Bell Lab in 1950s.They were studying electropolishing of silicon surfaces using aqueous solution of hydrogen fluoride (HF) found that, at low current densities, it results in a sponge-like structure. In the 1970s, researchers revealed the porous nature of material, but intended to use it only as a precursor for making low dielectric constant layers. Despite the observation of photoluminescence from porous silicon (PS) at cryogenic temperatures in 1984, wide attention to optical properties of porous silicon and other nanosilicon-containing system was only after reports on visible light emission at room temperature by Canham and blue shift of the absorption by Lehman and Gsele in 1990 [1].

In silicon science and technology the desire for the integration of optoelectronic devices with silicon microelectronics has led to the search for silicon-based structures that emit light with a high quantum efficiency value. Among the different approaches

used by researchers, the most recent is fabrication of silicon nanostructure (porous silicon, quantum dots, quantum wells, nanoclusters), which exhibit strong room temperature photoluminescence [2].This emission is observed only after a drastic size reduction and surface passivation of silicon and has been related to a quantum confinement and surface effect that occurs only when the particle size is smaller than the exciton radius in bulk (~5nm).The quantum confinement widens the and gap and extends the wave function in the momentum space, relaxing the k-selection rules [3,4].

There are two different mechanisms to study the electron-hole radiative recombination: the first assumes that the recombination occurs across the nanostructured gap, the other hypothesizes that the electron excited across the widened gap relaxes in the low-lying energy surface states [5, 6].In the latter case a small photoluminescence peak energy shift with the particle size is observed, whereas, in the other case the band gap energy scales as an inverse power of particle diameter. Next section focuses on the major applications.

1.2 Application of silicon nanostructure

Silicon is the most dominant material used for microelectronic devices in today's semiconductor technology. The desire to develop integrable devices with decreasing dimensions results in downscaling by nanostructuring of the base material. Crystalline silicon in its bulk appearance is commonly not taken into consideration as optical, magnetic or biomedical material but nanostructuring leading to a dramatic change of the properties compared to the bulk material is a method to enhance the functionality of silicon in nanotechnology. Light emitting properties occur due to quantum confinement effects and biodegradability as well as bioactivity of nanostructured silicon is observed and applied in many fields of biomedical and pharmaceutical research. Due to the dependence of refractive index modification on porosity porous silicon is interesting for optical applications including waveguide technology. The solubility in body fluids dependent on the porosity renders this material an interesting candidate for potential biomedical and pharmaceutical applications [7].

Silicon nanostructure with reduced dimensionality such as for example quantum wires, and quantum dots are attracting increasing attention both as the object of basic research and as promising materials for the fabrication of devices with new operational

capabilities that cannot be attained using traditional semiconductor materials. These materials are very important and promising in the manufacture light emitting diodes, high mobility transistors, sensors, monochromatic light source, wave guides, photonic studies, data storage devices and etc. The wide spread use of these materials and other related compound semiconductor materials light wave communication system has result in intensive research in to the growth of these materials using a number of techniques.

Silicon nanostructure with reduced dimensionality such as for example quantum wires, and quantum dots are attracting increasing attention both as the object of basic research and as promising materials for the fabrication of devices with new operational capabilities that cannot be attained using traditional semiconductor materials. These materials are very important and promising in the manufacture light emitting diodes, high mobility transistors, sensors, monochromatic light source, wave guides, photonic studies, data storage devices and etc. The wide spread use of these materials and other related compound semiconductor materials light wave communication system has result in intensive research in to the growth of these materials using a number of techniques.

In many applications of nanostructured materials, such as microelectronics, optoelectronics, and sensing the ability to fabricate nanostructures with a huge degree of regularity and uniformity is important in achieving tight control of their property [8].

1.3 Nanostructure fabrication methods

There are a variety of techniques that are capable of creating nanostructures with various degrees of quality, speed and cost. These approaches fall under two categories – “bottom-up” and “top-down” [9]. Bottom-up manufacturing involves the building of structures, atom-by-atom or molecule-by-molecule. Chemical synthesis, self-assembly and positional assembly are three main approaches in this method.

Top-down manufacturing involves starting with a larger piece of material and etching, milling or machining a nanostructure from it by removing materials. This can be done using techniques such as precision engineering and lithography. The prime example of the top-down approach is seen in the development integrated circuits (ICs), where the feature sizes of the components have decreased from several microns to dimensions less than 100nm [10]. Well-known products with nanometer dimensions include digital versatile discs (DVDs) and DVD-players, sensors, security lights and inkjet printers.

A diagram illustrating some of the types of materials and products that these two approaches are used for is shown in Fig. 1.

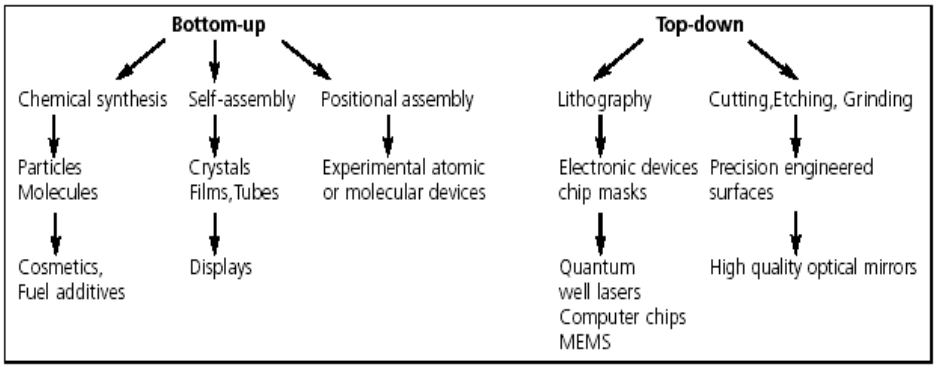

Figure 1.1The use of bottom-up and top-down techniques in manufacturing.

Although both approaches provide control over size, shape, composition, and surface chemistry, the bottom-up approach has more advantages. It facilitates the large scale, low-cost manufacturing of the dispersible nanomaterials for low temperature processing, deposition on plastic substrates, mixing with molecular and polymeric materials in coating and composites, and even interfacing with living organism for medical application.

The template method is one commonly used approach to obtain ordered array of one-dimensional nanostructures. As a well established nanotemplate, porous anodic alumina has been widely used to fabricate many kinds of nanowires and nanotubes; especially after the great improvement in pore regularity achieved using two step anodization process [8].Other methods for fabrication of ordered arrays include electron beam lithography, nanoimprint, and self assembly process. However, there are fabrications and application restriction for these methods, such as limited pattern area and low through put, high equipment capital costs, and limited classes of materials that can be pattern large areas of surface. Additionally, templates method allow for deposition of a wide range of materials [8].

Moving away from the trial-and-error recipes the field of nanomaterials chemistry has evolved a fundamental understanding of synthesis with control shape and size [11].

Silicon nanocrystallite can be produced by any of the following methods the vapor-liquid-solid (VLS) growth mechanism meant that grow from the gas phase by supplying Si vapor (physical vapor deposition (PVD) methods such as molecular beam epitaxy

(MBE) or electron beam evaporation (EBE), chemical vapor deposition (CVD), laser ablition etc. Figure 1 shows a schematic of the multicrystalline silicon layer stack on glass and the SiNW configuration after wet chemical etching [12]

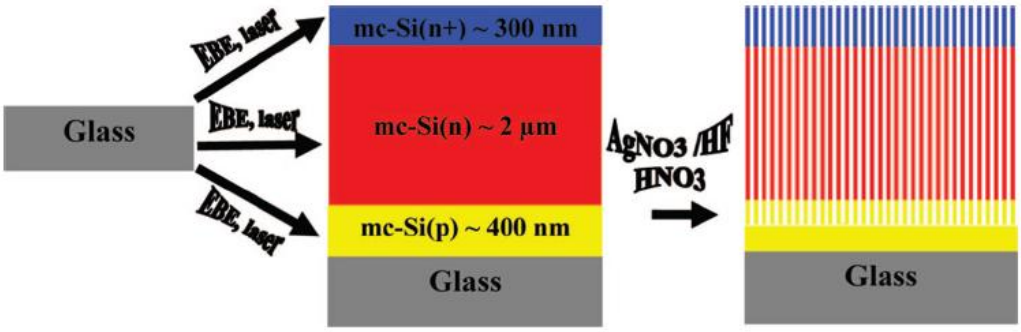

Figure 1.2 Schematic cross sectional view of the mc-Si p-n junction layer stack on a glass substrate (left) and the SiNWs after wet chemical etching (right).[12]

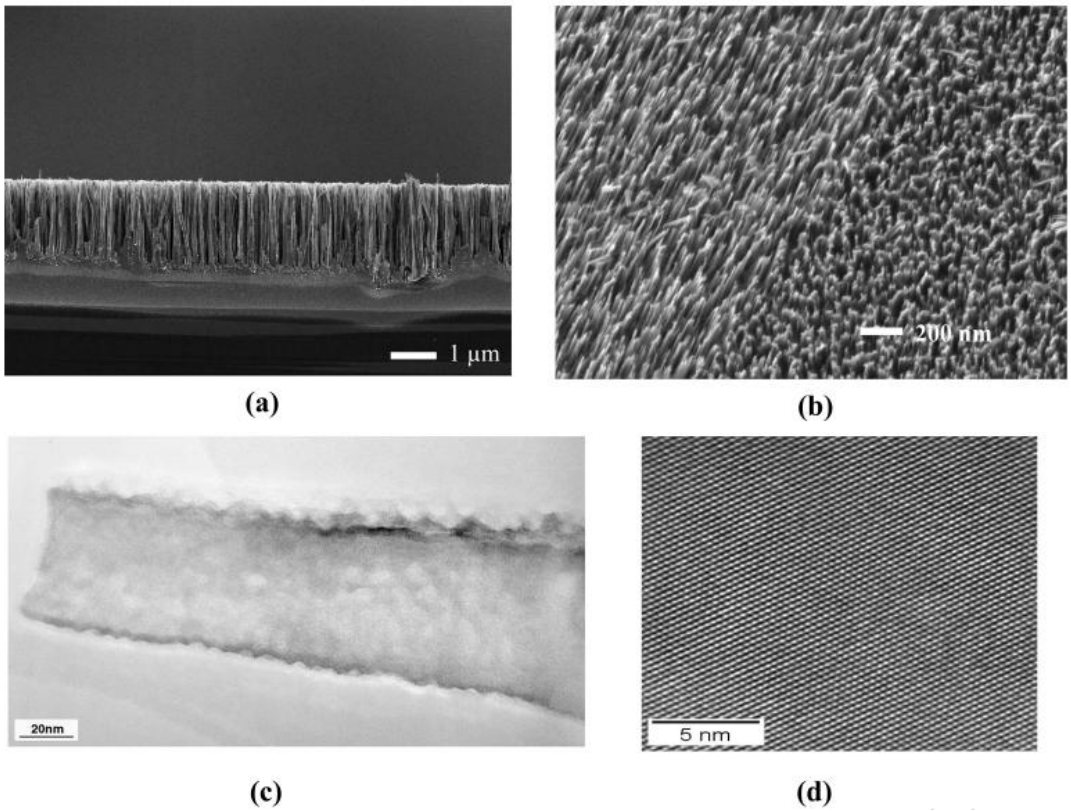

figure 1.3. *(a) Cross sectional SEM micrograph of the AgNO3/HF etched mc-p+nn+-Si layer on glass. (b) Planar SEM micrograph of SiNWs etched into grains of different orientation; the grain boundary in the staring mc-Si layer is clearly discernible. (c)*

Bright-field TEM image of a segment of a SiNW. The rough SiNW sidewalls are clearly visible. (d) High resolution TEM image of the SiNW with the lattice fringes clearly visible; the selected area is single crystalline [12]

1.4 Quantum confinement and optical properties

1.4.1 Quantum dots

Quantum dots (QDs) are nanometer scale "boxes" for selectively holding or releasing electrons. They are small physical devices that contain a ''tiny droplet'' of free electrons, small metal or semiconductor boxes that hold a specified number of electrons (QDs generally look more like pyramids than actual dots).QDs are grouping of atoms so small that the addition or removal of an electron will change its properties in a significant way. QDs are semiconductor structures where the electron wave function is confined in all three dimensions by the potential energy barriers that form the QDs boundaries. Specially, QDs are semiconductor structures that confine the electrons and holes to a volume of order of 20nm[3.]

Modern semiconductor processing techniques permit the artificial creation of quantum confinement (quantum confinement in all three special dimensions) of only few electrons; such a finite fermions QD systems have much in common with the atoms, yet they are man made structures, designed and fabricated in the laboratory.

The generalization of the Schrödinger equation in three dimensions:

$$E\psi(\mathrm{r}) = -\frac{\hbar}{2\mathrm{m}}\nabla^2\psi(\mathrm{r}) + \boldsymbol{V(r)\psi(r)} \quad \text{----------1.1}$$

The solution of the differential eq. (1.1) for a particle in 3D infinite trap of volume L^3 with impermeable walls with V(r) = 0 is given as:

$$\psi_n(x,y,z) = \left(\frac{2}{L}\right)^{\frac{3}{2}} \sin\left(\frac{n_x\pi x}{L}\right)\sin\left(\frac{n_y\pi y}{L}\right)\sin\left(\frac{n_z\pi z}{L}\right) \quad \text{----------1.2}$$

And the corresponding energy eigen value will be

$$E_n = \frac{\hbar^2\pi^2}{2mL^2}\left({n_x}^2 + {n_y}^2 + {n_z}^2\right) \quad \text{----------1.3}$$

Eqs. (1.2) and (1.3) are applicable to electron and hole states in semiconductor ''quantum dots''.

A ''hole'' (missing electron) in a full energy band behaves very much like an electron except that it has a positive charge, and tends to float to the top of the band, i.e. the energy of the hole increases oppositely to the energy of an electron. To create an electron

hole pair in semiconductors requires energy at least equal to energy at least equal to the energy gap E_g of semiconductor. The following figure shows the quantum dot embedded in SiO2.

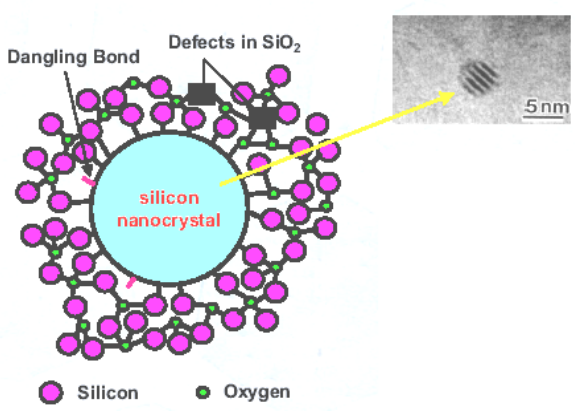

Figure1.4.Silicon nanocrystals embedded in SiO_2.

1.4.2 Quantum wires (nanowires)

Nanowires (also called quantum wires) are 1D molecular structure with electrical and/or optical properties. In order to have enhanced physical properties, the wires must be of small diameter, must have high aspect ratio (i.e. the ratio of length to thickness), and must be uniformly oriented. Nanowires are relatively easy to produce and can have different shapes. They are often thin and short ‘’threads’’ but also have other manifestations. The propagation of electromagnetic energy has been demonstrated along a noble metal stripes with band of a few microns, propagation has also been demonstrated along nanowires with sub wavelength cross sections and propagation length of a few micron. Metal nanowires can also be used to ‘’transmit’’ photons. The optical properties of metal nanowires can be optimized for particular wavelength of interest, and non-regular cross-sections and coupling between closely spaced nanowires allows a tunneling of optical response.

The term quantum wire describes a carrier confined in two dimensions say Y and Z to a small dimension d (wire cross-section d) and free to the form move along the length of the wire X (qualitatively this situation resembles the situation of the carrier moving along a carbon nanotube, or nanowire, although the details of the bound state wave functions are different).

The solution of eq. (1.1) in the case of quantum wire of a square cross-section is

$$\Psi_{nn}(x,y,z) = \left(\frac{2}{d}\right)\sin\left(\frac{n_y\pi y}{d}\right)\sin\left(\frac{n_z\pi z}{d}\right)exp(iK_xX)\text{----------1.4}$$

And the corresponding energy is

$$E_n = \frac{\hbar^2\pi^2}{2md^2}\left({n_x}^2 + {n_y}^2\right) + \frac{\hbar^2{K_x}^2}{2m}\text{ ----------1.5}$$

1.4.3 Quantum wells (QW)

A physical situation that often arises in semiconductor devices is a carrier confined in one dimension, say Z to a thickness d and free in two dimensions say X and Y this is called 2D bands or quantum wells. In this case the solution of eq. (1.1) will have the form

$$\Psi_n(x,y,z) = \left(\frac{2}{d}\right)^{1/2}\sin\frac{n_z\pi z}{d}\,exp(ik_zy)\text{---------- 1.6}$$

And the energy of the carrier in the n^{th} band [13, 14] is

$$E_n = \frac{\hbar^2}{2md^2}{n_z}^2 + \frac{\hbar^2{k_x}^2}{2m} + \frac{\hbar^2{k_y}^2}{2m}\text{ ----------1.7}$$

The following figure indicates the structure of the quantum dot, wire, and well.

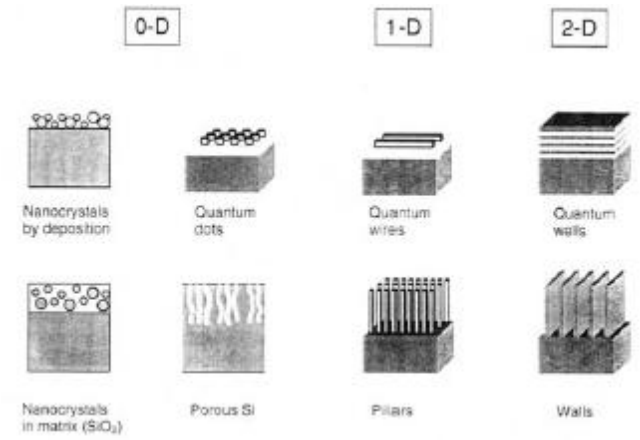

Figure 1.5 Schematic of low dimensional Structure

1.5 Optical property

Because of its 1.12 eV indirect band gap, silicon is characterized by a very poor optical radiative efficiency and only produces light outside the visible range. Until recent time

several attempts to improve this efficiency have been unsuccessful, but in the past decades room temperature visible photoluminescence has been observed from porous silicon surfaces prepared by chemical dissolution [15]. This observation has stimulated an intense experimental activity leading to promising results. In particular, electroluminescence has been reported during the anodic oxidation of porous silicon films and also during charge carrier's injection in rectifying junctions. The luminescence is often interpreted as resulting from the quantum confinement in small size crystallites of porous silicon. In effect, even if bulk silicon is poor emitter of light, silicon nanostructure (porous Silicon, quantum dots, quantum wells and nanoclusters) exhibit strong photoluminescence at room temperature. This is due to quantum size effect which leads to an increase (the blue shift) of the band gap of the crystallites compared to bulk silicon. As the size of nanoporous silicon becomes comparable to the Bohar exciton radius in bulk silicon, the quantum confinement widens the band gap. Thus, quantum confinement effect changes the indirect band gap nature of bulk Si to direct band gap in nanoporous silicon. Higher energy shift of energy levels with reduction of the size of semiconductor quantum dots by gaining the kinetic energy due to spatial confinement of the electrons by a potential barrier is often referred to as a quantum confinement effect. The electronic states of silicon nanocrystallites (Si-nc) as compared to that of bulk Silicon are dramatically influenced both by quantum confinement (QC) and by the enhanced role of state- and defects-at the surface. The effect of quantum confinement is a rearrangement of the density of electronic states in energy as direct consequence of volume shrinking in one, two or even three dimensions, which can be obtained, respectively, in quantum wells, wires, and dots. The Modification of material properties, especially optical one, by reducing the dimension makes nanostructuring of a semiconductor an alternative way to look for new material. In recent years spectroscopic studies show that an increase of the band gaps [16] and the oscillator strength with decreasing size of the nanocrystallites. As a result, despite the fact bulk Silicon is a very inefficient light emitter, low dimensional Silicon shows light amplification characteristics, non linear optical effect as well as visible light emission. The effect of quantum confinement is changing the indirect band gap nature to direct band gap. The direct band gap nature has more advantage in that, it is not phonon assisted. Direct gap transition is K-conserving so that there is no wastage of

energy. This is not in fact observed in indirect transition. The following figure shows the transition of electron from valence band to conduction band of semiconductor silicon.

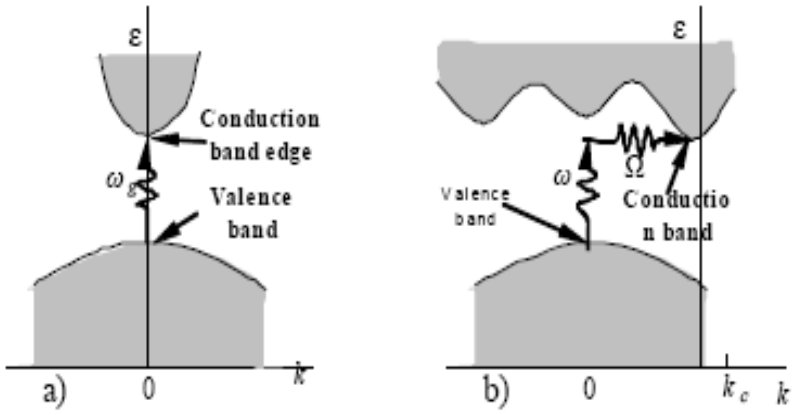

Figure1.6 Schematic representation of direct (a) and indirect (b) band gap semiconductor

1.6 Photoluminescence

Silicon nanocrystal (Si-nc) is a topic of great interests in the field of optelectronics because of its high quantum efficiency of photoluminescence (PL) and relatively large nonlinear optical responses. The large nonlinear optical response has been reported in various forms of Si-ncs such as porous Si prepared by electrochemical etching Si-nc doped SiO*x*N*y* deposited by plasma enhanced chemical vapor deposition (PECVD), Si-ncs doped SiO2 prepared by cosputtering, laser ablated Si-ncs deposited on quartz substrate, and so on. In these literatures, dependence of the nonlinear optical response on the size and volume fraction of Si-ncs has been studied in detail. Although the origin of the large nonlinear optical response is still not fully clarified, the quantum confinement effects are often believed to be responsible [17].

Very recently many attempts have been made to produce quasi-direct-gap semiconductor nanostructures made from indirect -gap semiconductors and a great deal of research effort is focused on nanometer size crystallites or quantum dot made from Si. Strong Photoluminescence at room temperature from Si nanostructures with diameters less than

5 nm has attracted much attention from fundamental physics viewpoint and because of the potential application to optical devices.

There exist two classes of explanation for the origin of visible PL in porous silicon:(1) the quantum confinement model in which luminescence is due to electronic confinement in the columnar like (or dot like) structure of porous silicon, and (2) the chemical model in which the large surface area presented by porous silicon support luminescing siloxenes. For H-terminated, photoluminescence spectral shows continuous shift of peak energy from the bulk band gap to the visible region with a good agreement with the quantum confinement effect, whereas the photoluminescence spectra of oxidized surface porous silicon are confined to a specific region [18]. Generally, silicon nanocrystallites grown by different methods exhibit strong photoluminescence in the red region and progressively shift towards the blue when the mean size decreases. Depending on the size, the photoluminescence of silicon nanocrystals can be tuned from the near infrared (1.38 eV) to theultraviolet (3.02 eV) i.e. as the size of a silicon nanocrystallite structure decreases, the band gap of the material increases due to the quantum confinement effect [Fig (1.2)].

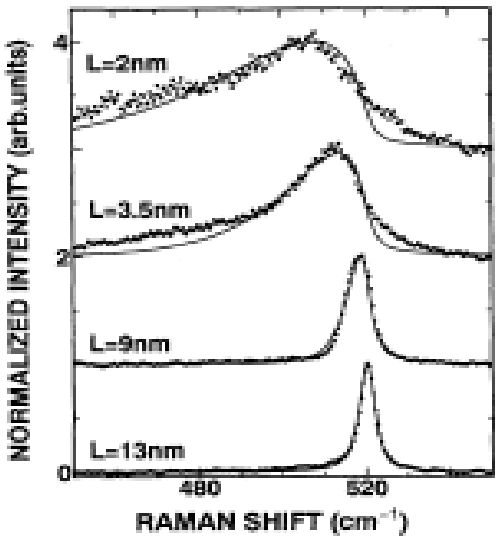

Figure 1.7 Raman spectra of free-standing porous Silicon film compared with the spectra calculated for a sphere with diameter L (solid lines).

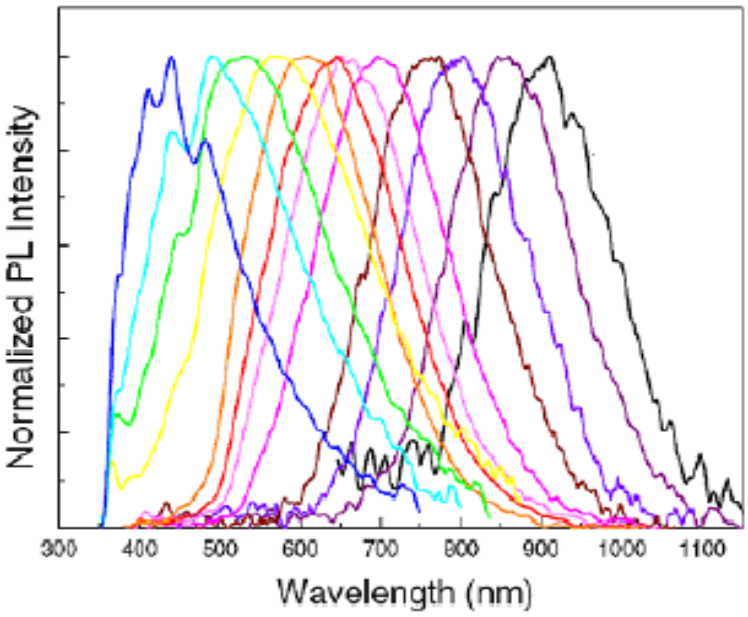

Figure 1.8: Room temperature photoluminescence spectra of silicon nanocrystallites. The peak position can be controlled by the appropriate adjustment of the nanocrystallites Size [19].

Fig. 1.8 shows a room-temperature photoluminescence spectrum obtained from various sized silicon nanocrystals, where the tuning of the photoluminescence emission from 410 to 900 nm is possible by controlling the size of the silicon nanocrystallite and, as a result, the emission color can be changed by controlling the size of the nanocrystallite. For example, nanocrystallite sizes corresponding to red, green, and blue emission are 4.6, 3.1, 2.7 nm, respectively [19].

1.7 Objective of the thesis

Our main objective here in this thesis is to study and investigate effect of size reduction and surface passivation on the optical properties of silicon nanostructure.

Specifically, we investigate the effect of size and surface passivation on

Band gap energy and photoluminescence of silicon nanostructure where the silicon nanostructure is passivated with hydrogen and oxygen by analytically estimating the optical parameter of nanoporous silicon at different size and passivation (i.e. oxygen and hydrogen passivation).

1.8 Methodology

Our method starts with the developing model that can describe the mechanism of light emission from nanosilicon (spherical crystallites). This model is based on the quantum mechanical modeling of the nanostructure and uses the quantum mechanics equestions and fit our model calculation to the experiments taking data from simulation based on Empirical Pseudo Potential Approximation (EPPA) and Tight-binding theory. We use matlab to see the results of our model.

1.9 Thesis outline

In this thesis we study the role of surface chemistry in modifying the optical properties of silicon nanostructure by estimating the photoluminescence band energy for pure and passivated nc-Si as a function of size of the dot and photon energy as well as size distribution. The thesis is organized into five chapters. Chapter 2 discusses the density of states of confined systems and theoretical methods on nc-Si. Chapter 3 discusses the different models used to explain the optical properties of silicon nanostructures. Chapter 4 contains our model that is formulated to explain the optical properties. Chapter 5 contains result and discussion, and chapter 6 gives the summary and conclusion.

Chapter Two

Density of states and theoretical methods

2.1 Density of state

In order to characterize the physical properties like optical transitions, charge transport etc., the information about the density of states is very crucial [20]. The density of states depends on the dimensionality of the system and the energy versus the corresponding wave vector dispersion relation for the system at hand [21].

A general expression for the density of states valid for all types of materials is as a sum delta functions

$$g(E) = \sum_{E_i} \delta(E - E_i) \text{----------} 2.1$$

Or

$$g(\omega) = \sum_{k} \delta(\omega - \omega_k) \text{----------} 2.2$$

For parabolic approximation of the energy versus the corresponding wave vector dispersion relation for the electron or hole we can take a simpler form. Therefore, for a three-dimensional bulk material, the DOS is defined as the number of available electronic states per unit volume per unit energy at energy E and is given by

$$g(E) = \frac{\sqrt{2} m_e^{3/2}}{\pi^2 \hbar^3} E^{1/2} \text{----------} 2.3$$

Passing from three-dimensional bulk to two-dimensional structures, (so called quantum well) the carrier movement is restricted to a plane. Such two-dimensional systems include thin films, layer structures and super lattices. Now the DOS is modified to the number of available electronic states per unit area per unit energy and is given by

$$g(E) = \frac{m_e}{\pi^2 \hbar^2} \text{----------} 2.4$$

Further reduction in the dimensionality of the system ends up in a quantum wire. Examples of such one-dimensional structures include nanotubes, semiconductor nanowires, and nanorods. For a quantum wire the DOS is defined as the availability of electronic states per unit length per unit energy and is given by

$$g(E) = \frac{\sqrt{2}m_e^{-\frac{1}{2}}}{\pi h} E^{-\frac{1}{2}} \quad \text{----------2.5}$$

Finally, for a zero dimensional system (QD), the confinement is along all three dimensions and the DOS becomes a delta function. Fig. 2.1 schematically shows the modifications in the DOS as a function of dimension.

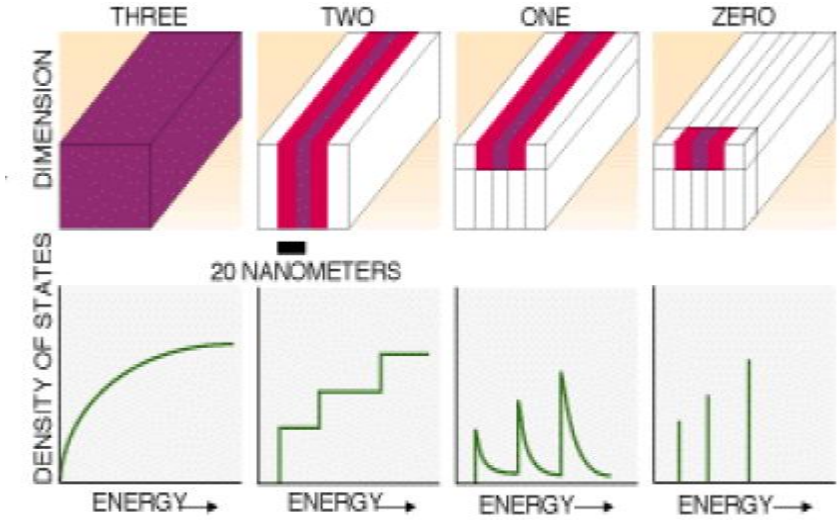

Figure 2.1.Density of states for various geometries of semiconductor materials: (a)3-D bulk, (b) quantum well, a 2-D structure, (c) quantum wire, a 1-D structure, and (d) quantum dot, a 0-D entity. The dotted line in (a) is the thermal distribution of carriers.

Transformation from a 3-D bulk system to a 2-D thin film changes the DOS from a continuous parabolic dependence to a step like dependence. This is due to the quantization of carrier motion in the thickness direction. Consequently the optical absorption edge is shifted to higher energy with respect to the bulk and above the absorption edge; the spectrum is stepped rather than smooth [22].

2.2 Band Theory

Optical transitions in atoms and molecules occur between discrete levels. Semiconductors (bulk) are however characterized by bands and the study of optical processes in semiconductors invariably requires complete knowledge of band structure [23]. The band theory of solids, including semiconductors, is a many-particle theory involving all

electrons and ions and their mutual interactions. This many-body problem may be reduced under various approximations to a single-electron problem that predicts most of the important features. In the one electron theory an electron is assumed to exist in a periodic potential and the solution of Schrödinger's equation with periodic boundary conditions yields different bands that are separated from each other by a forbidden band gap.

We note that in optical transitions from the valence band to the conduction band the electrons involved cover an energy interval of a small fraction of an electron Volt (eV).

A prediction of the quantum confinement model is that the energies of the valence band (VB) and conduction band (CB) edges are shifted relative to the bands of bulk silicon, leading to an increased energy gap. This is confirmed from the comparison of the band edge spectra of the nanocrystal with that of the bulk.

According to the quantum confinement theory, electrons in the conduction band and holes in the valence band are confined spatially by the potential barrier of the surface or trapped by the potential well of the quantum box. Because of the confinement of both the electrons and holes, the lowest energy optical transition from the valence to the conduction band increases in energy, effectively increasing the energy gap (E_g). The sum of the kinetic and potential energy of the freely moving carriers is responsible for the E_g expansion and therefore, the width of the confined E_g grows as the characteristic dimensions of the crystallite decreases.

Recent bulk sensitive and element specific soft X-ray fluorescence measurements of the VB of silicon nanoclusters also show a shift in the VB maximum that is comparable to the photoemission result [23].

2.3 Theoretical methods

A significant part of condensed matter physics and chemistry would be solved if the electronic structure of atoms, molecules and solids could be determined exactly. This however, needs a formidable for two main reasons. Firstly, electron in matter must be treated using the laws of quantum mechanics rather than classical physics. The quantum

length scale is set by Planck's constant h, and the onset of quantum effects occur when the de Broglie wave length (λ) of a particle given by

$$\lambda = \frac{h}{p}$$ ----------2.6

is comparable to the average inter particle separation. Rearranging the energy momentum equation $E = \frac{p^2}{2m_e}$ the electronic thermal energy relationship E ~ k_BT, leads to a relation for the de Broglie wave length of an electron given in terms of electron mass me and temperature T,

$$\lambda = \frac{h}{\sqrt{2m_e k_B T}}$$ ----------2.7

For solid state systems the average inter electron separation is usually represented by the Wigner-Seitz radius r_s, which is the radius of a sphere whose volume encloses a single electron in the system, and is normally written in terms of the Bohr radius, a_o ~0.529 × 10^{-10}m = 0.529A^o

$$\frac{r_s}{a_o} = \left(\frac{3}{4\pi} n_o\right)^{1/3}$$ ----------2.8

Where n_o is the average electron density. For most systems of interest r_s typically ranges from 0.1 up to 10 nm, which means that the electron de Broglie wave length is larger or comparable to the average separation up to T ~10^4K, according to relation (2.7). Therefore within this temperature range the de Broglie wave length of the electrons overlap and the interactions between the electrons become quantum mechanically correlated. The second problematic issue concerns the number of electrons that are involved the coupling of the electrons due to de Broglie wavelength overlap renders an analytical solution impossible for systems with more than one electron, and the complexity grows dramatically with ,increasing electron number. It is for these reasons that the electrons structure of matter is known as quantum many-body problem. Quantum many body problem is usual within the realm of theoretical physics because the equations required for an exact solution are known. The properties of any time independent quantum system can be determined by solving the Schrödinger equation,

$$\hat{H}\psi(\overrightarrow{r_1}, \overrightarrow{r_2}, \dots, \overrightarrow{r_n}) = E\psi(\overrightarrow{r_1}, \overrightarrow{r_2}, \dots, \overrightarrow{r_n})$$ ----------2.9

Where $\hat{H}$, $\psi(\overrightarrow{r_1}, \overrightarrow{r_2}, \ldots, \overrightarrow{r_n})$, and E are the Hamiltonian, many-body wave-function and total energy of the system. Matter consists of electron and nuclei interacting with each other coulombically, consequently the Hamiltonian for any such system is given by,

$$\hat{H} = -\sum_{i=1}^{M} \frac{\hbar^2}{2mz_i} \nabla_{R_i}{}^2 - \sum_{i=1}^{N} \frac{\hbar^2}{2m_e} \nabla_{r_i}{}^2 + \frac{1}{4\pi\varepsilon_o} \sum_{i}^{M} \sum_{j>i}^{M} \frac{Z_i Z_j}{|\overrightarrow{R_i} - \overrightarrow{R_j}|} - \frac{1}{4\pi\varepsilon_o} \sum_{i=1}^{N} \sum_{j=1}^{M} \frac{eZ_j}{|\overrightarrow{r_i} - \overrightarrow{R_j}|} +$$

$$\frac{1}{4\pi\varepsilon_o} \sum_{i=1}^{N} \sum_{j>i}^{N} \frac{e^2}{|\overrightarrow{r_i} - \overrightarrow{r_j}|} \text{----------} 2.10$$

Where M and N are the number of nuclei and electrons in the system, m_Z, Z and R are the mass, charge and position of the nuclei, m_e and e are the mass and charge of an electron, and r represents the position of the electrons. The first two terms in (2.10) are the kinetic energy contributions from the nuclei and the electrons respectively, and the rest are columbic potential energy terms arising from ion-ion repulsion, ion-electron attraction and electron-electron repulsion respectively. Although in principle everything is known exactly, the Schrödinger equation (2.9) with this Hamiltonian is simply too difficult to solve directly. Hence, the quantum many-body equation centered upon finding intelligent approximations to the Hamiltonian (2.10) and the many-body wave-function ψ that retain the correct physics and are computationally tractable to solve.

2.3.1 The Born-Oppenheimer theory

This is the first of a series of approximations that is used to solve the complexity of the electronic movements in a solid. Born and Oppenheimer recognized that in most cases the nuclear and electronic degrees of freedom can be decoupled since they exhibit vastly different dynamics: the nuclei are of order ~10^3 times heavier than the electrons and so are considered to be stationary with respect to the electrons. The electrons therefore move within fixed external potential due to the nuclei. Within Born-Oppenheimer approximation the complexity of full many-body Hamiltonian Eq. (2.10) reduces to electronic Hamiltonian,

$$\hat{H} = -\sum_{i=1}^{N} \frac{\hbar^2}{2m_e} \nabla_i{}^2 - \frac{1}{4\pi\varepsilon_o} \sum_{i=1}^{N} \sum_{j=1}^{M} \frac{Z_j e}{|\overrightarrow{r_i} - \overrightarrow{R_j}|} + \frac{1}{4\pi\varepsilon_o} \sum_{i=1}^{N} \sum_{j>i}^{N} \frac{e^2}{|\overrightarrow{r_i} - \overrightarrow{r_j}|} \text{----------} 2.11$$

Solving the Schrödinger equation with this Hamiltonian is however still too complex for most cases. Since the many-electron wave function contains 3N variables, which for solid contain N~10^{26} electrons, is simply an intractable number of degrees of freedom.

2.3.2 First principle modeling of nanostructures

Among the various theoretical tools for investigating microscopic material properties, ab initio (first principles) methods based on density functional theory decades in terms of accuracy, reliability, and efficiency [24]. The application of these methods to nanostructures and pseudo potentials have had a very good track record over the last two to investigate their structural, electronic, and optical properties has, however not been straight forward due to the large computational demand and new physics inherent in the nanometer and sub-nanometer size region.

2.3.3 Density functional theory (DFT)

Density functional theory (DFT) provides a tractable way of solving the quantum equations of motion for a system of interacting electrons under an external potential, such as the electron-ion interaction potential in solid [24]. The proper choice of the potential appearing in the one-electron Schrödinger equation

$$-\frac{\hbar^2}{2m}\nabla^2\psi(\vec{r}) + U(\vec{r})\psi(\vec{r}) = \epsilon\psi(\vec{r})$$----------2.12

is a suitable problem [25]. Underlying this problem is the equation of how best to describe electron in a metal correctly by so elementary an equation as (2.12). In 1964, Hohenberg and Kohn proved a famous theorem, which states that the ground state energy of an electron gas with a non-degenerate ground state under an external potential is a unique function of the electron charge density $\rho(\vec{r})$ and that this energy functional assumes its minimum value (ground state energy) for the correct (ground state) $\rho(\vec{r})$ [26]. A year later, Kohn and Sham expressed this charge density in terms of orthonormal single particle wave functions $\psi(\vec{r})$ [27].

$$\rho(\vec{r}) = -e\sum_i|\psi_i(\vec{r})|^2$$----------2.13

Where the sum extends over all occupied one electron levels in solid

A more accurate calculation of electronic properties of a metal should start with the Schrödinger equations for the N-particle wave function of all N electrons in the metal, ψ_i

$$H\psi = \sum_{i=1}^{N}\left\{-\frac{\hbar^2}{2m_e}\nabla_i^{\,2} - \frac{1}{4\pi\varepsilon_o}\sum_{j=1}^{M}\frac{Z_j e}{|\vec{r}_i-\vec{R}_j|}\right\}\psi + \frac{1}{4\pi\varepsilon_o}\sum_{i\neq j}\frac{e^2}{|\vec{r_i}-\vec{r_j}|}\psi = E\psi$$----------2.14

Where the total eigen value E is equal to:

$$E = \sum_{i=1}^{N} \left\{ -\frac{\hbar^2}{2m} \nabla^2{}_i - \frac{1}{4\pi\varepsilon_o} \sum_{j=1}^{M} \frac{Z_j e}{|\vec{r_i} - \vec{R}|} \right\} + \frac{1}{4\pi\varepsilon_O} \sum_{i \neq j} \frac{e^2}{|\vec{r_i} - \vec{r_j}|} \text{----------2.15}$$

Here the negative potential-energy term represents the attractive potentials of the bare nuclei fixed at the points R of Braves lattice, and the last term represents the interaction of electrons with each other. One has no hope of solving an equation such as (2.14) easily. Further progress requires some simplifying physical idea. One such idea is suggested by asking what choice of $U(\vec{r})$ would make the one electron equation (2.12) least unreasonable. Evidently $U(\vec{r})$ should include the potential of the ions:

$$U^{ion}(\vec{r}) = -Ze \sum_R \frac{1}{|\vec{r} - \vec{R}|} \text{----------2.16}$$

In addition we should like $U(\vec{r})$ to incorporate (at least approximately) the fact that the electron feels the electric fields of all other electrons. If we treat the remaining electrons as a smooth distribution of negative charge with charge density ρ, the potential energy of the electrons in their field would be:

$$U^{el}(\vec{r}) = -e \int dr' \, \rho(\vec{r}) \frac{1}{|\vec{r} - \vec{r'}|} \text{----------2.17}$$

Letting $U(\vec{r}) = U^{ion} + U^{el}$ we arrive at the one-electron equation:

$$-\frac{\hbar^2}{2m} \psi_i(\vec{r}) + U^{ion} \psi_i(\vec{r}) + \left\{ e^2 \sum_j \int dr' \, |\psi_j(\vec{r})|^2 \frac{1}{|\vec{r} - \vec{r'}|} \right\} \psi_i(\vec{r}) = \epsilon_i \psi_i(\vec{r}) \text{----------2.18}$$

The set of equation (2.18) called Hartree equation and in a more compact form:

$$\left\{ -\frac{\hbar^2}{2m} \nabla^2 + V_{eff}[\vec{r}, \rho(\vec{r})] \right\} \psi_i(\vec{r}) = \epsilon_i \psi_i(\vec{r}) \text{----------2.19}$$

Where

$$V_{eff.}[\vec{r}, \rho(\vec{r})] = U^{ion} - e \int \frac{\rho(\vec{r'})}{|\vec{r} - \vec{r'}|} dr' \text{----------2.20}$$

Due to the dependence of Veff. on $\rho(\vec{r})$, which depends on the solutions $\psi_i(r)$ of the Schrödinger equation, equations (2.13), (2.19), and (2.20), known as the Kohn-Sham (KS) equations, have to be solved self-consistently.

2.3.4 Ab intio pseudo potential

This method, which can be implemented in both momentum and real space, has a very good track record for investigating structural, electronic, optical properties of a large variety of materials. The pseudo potential method relies on the separation (in both energy and space) of electrons into core and valence electrons and that most physical and chemical properties of materials are determined by valence electrons in the interstitial region. One can therefore combine the full ionic potential with that of the core electrons' to give an effective potential (called the pseudo potential), which acts on the valence electrons only. On top of this, one can also remove the rapid oscillations of the valence wave functions inside the core region such that the resulting wave function and potential are smooth. The pseudo potential model treats matter as a sea of valence electrons moving in a background of frozen ion cores. The cores are composed of nuclei and inner inert electrons.

There are various advantages of the pseudo potential method. By eliminating the core electrons from the problem, the number of particles for which the KS equations to be solved is decreased. For example, a pseudo potential calculation for bulk silicon (with 10 core and 4 valence electrons) requires the calculation of 4 occupied bands at each k-point, while an all-electron approach would require the calculation of 14 occupied bands. More importantly, the smooth spatial variation of the pseudo potential and pseudo wave function allows the use of computationally convenient and unbiased basis, such as plane wave basis sets or grids in space.

The difficulty with approximating valence wave functions by a few plane waves everywhere in space (as in the nearly free electron method) is that this hopelessly fails to produce the rapid oscillatory behavior required by exclusive principle in the core region.

2.3.5 Free electron gas model

Perhaps the simplest description of condensed matter system is to imagine non-interacting electrons as contained within a cube of edge L. The free particle Schrödinger equation is obtained by setting the potential zero [28].

$$H = \frac{p^2}{2m} = -\frac{\hbar^2}{2m}\vec{\nabla}^2 \text{----------2.21}$$

Where

$$\nabla^2 = \frac{\partial^2}{\partial x^2} + \frac{\partial^2}{\partial y^2} + \frac{\partial^2}{\partial z^2} \text{----------2.22}$$

Which implies

$$-\frac{\hbar^2}{2m}\left(\nabla^2 = \frac{\partial^2}{\partial x^2} + \frac{\partial^2}{\partial y^2} + \frac{\partial^2}{\partial z^2}\right)\psi_k(\vec{r}) = \epsilon_k\psi_k(\vec{r}) \text{----------2.23}$$

For the electrons confined to a cube of edge L, the wave function is the standing wave:

$$\psi_n(\vec{r}) = A\sin\left(\frac{n_x\pi x}{L}\right)\sin\left(\frac{n_y\pi y}{L}\right)\sin\left(\frac{n_z\pi z}{L}\right) \text{----------2.24}$$

Where A is the amplitude, and n_x, n_y, n_z, are positive integers.

Chapter Three

Energy gap and Photoluminescence model for nanocrystalline silicon

3.1 Energy gap of nano-structures

Most of material properties, such as the dielectric function and optical transitions, depend on energy-gap between the conduction band and the valance band of the material thus altering the energy gap may significantly alter the materials optical properties, more interestingly in the last decade it was proposed that the band gap is a function of porous silicon nanoclusters diameter (size) which eventually lead to the fact that altering the energy gap may significantly alter the materials optical properties. In this topic our main objective will be to investigate how the material properties specially optical one are related to the size of porous silicon nanocluster. As we all know because of its 1.12 eV indirect band gap silicon is characterized by a very poor optical radiative efficiency and only produces light outside the visible range. But after many investigations it has been observed that quantum confined nano-silicon structures are direct band gap material which show zero phonon transition reflected in the Raman spectra. This is due to quantum size effect which leads to an increase (the blue shift) of the band gap of the crystallites compared to bulk silicon. As the size of nanoporous silicon becomes comparable to the Bohar exciton radius in bulk silicon, the quantum confinement widens the band gap. Thus, quantum confinement effect changes the indirect band gap nature of bulk Si to direct band gap in nanoporous silicon which lead to a very good optical radiative efficiency. However, this cannot be explained only by quantum confinement effects also effects such as structural changes, lattice contractions and surface passivation can change the band-gap of the material. And several models have been proposed in order to describe band structure of clean, oxygen and hydrogen passivated sample, for instance tight-binding method, pseudopotential method and the effective mass approximation (EMA) are few of them. In their remarkable work Zunger et al [29] using tight-binding method, Tripathy et al [30] and Ghoshal et al [31] using local pseudopotential method calculated the band gap energy as a function of diameter (size) for clean surface silicon nanoclusters at room temperature and found approximately the gap as:

$E_g^{nano}(L) = E_g^{bulk} + \frac{c_1}{L^{\alpha_1}}(eV)$----------3.1

Where: $E_g^{nano}(L)$, $E_g^{bulk}$and L in (nm) are the band gap energy of silicon nanocrystal, bulk silicon band gap energy at room temperature and diameter (size) of the silicon nanocrystallite respectively. Tripathy et al also calculated band gap energy for hydrogen passivated silicon nanocrystals using local pseudopotential method at room temperature as:

$E_g^{nano}(L) = E_g^{bulk} + \frac{c_2}{L^{\alpha_2}}(eV)$----------3.2

Where the calculated band-gap energy for oxygen-passivated silicon nano-crystals using the local pseudo-potential method is given by:

$E_g^{bulk}(L) = E_g^{bulk} + \frac{c_3}{L^{\alpha_3}}(eV)$----------3.3

For all these materials, the variation of the band gap follows roughly the same kind of law.

$E_g^{nano}(L) = E_g^{bulk} + \frac{c}{L^{\alpha}}(eV)$----------3.4

The value of c and α differ depending on the type of the crystalline silicon. That is whether the surface of the crystalline silicon is passivated or not. Even the type of passivation determine the value of c and α. Furthermore, from this expression it is evident that the energy necessary to generate an electron-hole pair increases by decreasing the size of the system and we can also see that surface passivation plays an important role in increasing the band-gap of the nano-crystals. In general, fig. 3.1 illustrates the calculated band-gap variation as a function of diameter. In the next sections we will discuss how the optical properties of nano-silicon namely photoluminescence change with the band gap of the silicon nanostructure.

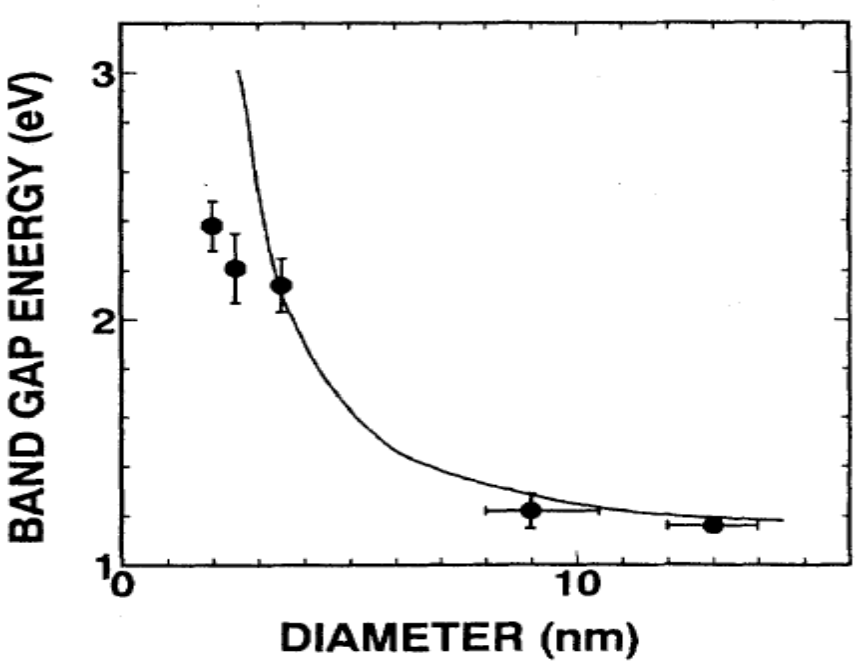

Figure 3.1: Band gap as a function of size (Diameter)

3.2 photoluminescence from nanocrystalline silicon

Photoluminescence (abbreviated as PL) is a process in which a substance absorbs photons (electromagnetic radiation) and then radiates photons back out. Quantum mechanically, this can be described as excitations to a higher energy state and then a return to a lower energy state accompanied by the emission of a photon. This is one of many forms of luminescence (light emission) and is distinguished by photo-excitation (excitation by photons), hence the prefix photo. The period between absorption and emission is typically extremely short, in the order of 10 nanoseconds. Under special circumstances, however, this period can be extended into minutes or hours. Ultimately, available chemical energy states and allowed transitions between states (and therefore wavelengths of light preferentially absorbed and emitted) are determined by the rules of quantum mechanics. A basic understanding of the principles involved can be gained by studying the electron configurations and molecular orbital of simple atoms and molecules. More complicated molecules and advanced subtleties are treated in the field of computational chemistry [32].

Semiconductor materials have been widely studied in recent years for their potential use in nonlinear optical devices. Silicon is the dominant material in present-day microelectronics technology; however, bulk crystalline silicon is not known to be the nonlinear material of choice due to the long lifetime of its carriers and indirect band gap in the near infrared (IR) spectral region, with very low emission efficiencies (one photon emitted for every 107 photo-generated electron-hole (e-h) pairs). The main reason that Si-based photonics has lagged behind microelectronics is the lack of practical Si light sources, such as efficient Si light-emitting diodes (LED) and injection lasers. Light emission in bulk Si is phonon-mediated, with a very low probability because the spontaneous recombination lifetimes are in the millisecond range. The competitive non-radiative rates are much higher than the radiative ones, and most of the e-h pairs recombine non-radiatively. The quantum efficiency for Si luminescence is very low. Bulk Si does not have lasing action because the fast non-radiative processes such as Auger or free-carrier absorption strongly prevent population inversion at the high pumping rates needed to achieve optical amplification. However, at nanosize dimensions, silicon exhibits sizeable nonlinear effects. The idea of exploiting Si for light-emitting devices is appealing because it leads to the possibility of fabricating light-emitting devices compatible with Si-based optoelectronic integrated circuits. The discovery of visible PL at room temperature from electrochemically etched porous silicon has prompted enormous interest in nanocrystalline silicon (nc- Si) structures for their possible applications in opto- electronics integration. Most of the present day research on photonic applications of Si is directed towards developing Si-based nanomaterials that emit light in the visible range efficiently and predictably.

It is believed that light emitting Si-devices would not only be cheaper than those

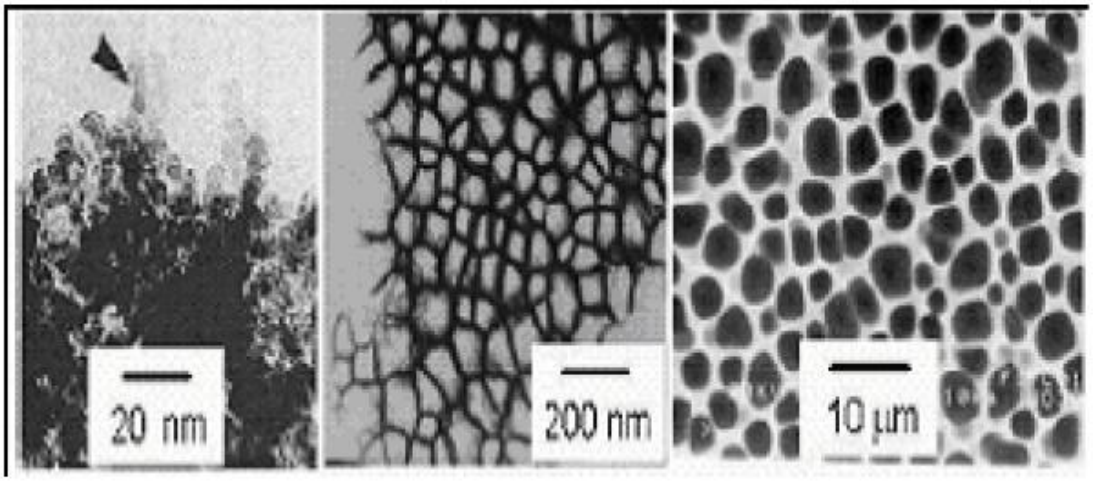

Figure 3.2: Different p-Si structures: nanoporous (left), meso-porous (middle) and Macro-porous (right). Made of compound semiconductors, but could also be integrated onto traditional circuits.

Silicon nanoclusters (porous as well as nano-crystallites) have been the subject of many experimental and theoretical investigations for nanoscale fabrication and Miniaturization of microelectronic devices. Porous Si is made up of interconnected branches of nanometer size Si nanocrystals embedded in an amorphous matrix, which can be described in terms of quantum wires and quantum dots. At present, there is a common understanding that nanometer sized Si clusters have largely different physical and chemical properties from that of bulk Si. Recently, some efforts have been made to build silicon nanotubes or nanowires, as well as stable Si quantum dots based on the silicon clusters. Depending on the sizes of pore diameter, p-Si is classified as nanoporous (pore size less than 5 nm), meso-porous (pore size ~5 − 50nm), and micro-porous (greater than 50 nm) as shown in Fig.3.2 [33]. Porous Si has proved to be one of the most promising candidates with regards to luminescence among all other Si-based materials studied so far. It was the first and it is still the least expensive material in use, for which the optical properties of Si-NC are studied. The fabrication procedure for p-Si is very flexible.

Porous Si emits light at room temperature in the visible range, with quantum efficiencies as high as 10 percent (one photon emitted for every 10 photo-generated electron-hole pairs).

3.3 Models for photoluminescence

There is much debate about the PL mechanisms of the nanoscale Si/SiO_2 systems containing oxidized porous Si and nanoscale-Si-particle (NSP) embedded in Si oxide deposited by chemical vapor deposition, sputtering or Si-ion implanting in to Si oxide. Canham reported strong visible PL from porous silicon at room temperature and suggested the quantum confinement model for its mechanism in 1990. Since then there has been a long debate on the PL mechanism of P-Si. Some literatures mentioned that more than one type of mechanism models are needed in interpreting PL from P-Si. We describe the most commonly mentioned PL mechanism models, Quantum Confinement Model (QCM), Surface State Effect (SSE), and Quantum Confinement Luminescence Center Model (QCLCM).

3.3.1 Quantum Confinement Model

The quantum confinement model (QCM) is the first mechanism model suggested to explain the visible light emission in porous Si. In this model, the light emission process itself was assumed to be the result of carrier recombination within quantum confined Si-ncs, (i.e. both the optical excitation and recombination takes place inside the nanosilicon particle) and the energies of the resultant PL were expected to inversely scale with the particle size. This is similar to the diagram in Fig. 3.3 but in this case the emission energy E_g would be replaced by E_{QC}, the energy due to quantum confinement effect, which could be significantly above 1.12eV, due to the quantum confinement of the carriers.

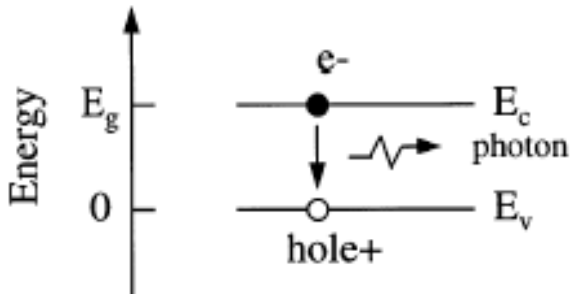

Figure 3.3 .Schematic representation of one of the possible optical transitions leading to light emission in semiconductor, band-to-band recombination [33].

Several key factors have been used to support this emission model. These include the presence of intense visible light in Si, the PL blue shift with increased etching, the multi-exponential PL decay characteristics, the low temperature Si phonon replicas reported in PL spectrum and the particle size dependent absorption behavior. We will not address all these issues here; however, the following section is devoted to discuss some of these factors along with the shortcomings of the dominant QC model. Since the report by Canham [15] of an intense red PL from P-Si, calculations have been reported suggesting that the optical gap could lead to sizeable blue shift due to QC, and oscillator strength would increase significantly, leading to much more efficient PL. In P-Si, Si particle sizes below 5nm would enhance the oscillator strength, as well as produce a sizeable blue shift of optical gap from 1.12eV, possibly in the range of 1.5 to 1.9eV [34]. Figure 3.4 shows the effect of quantum confinement on band gap energy and the corresponding light emission as the size is decreased.

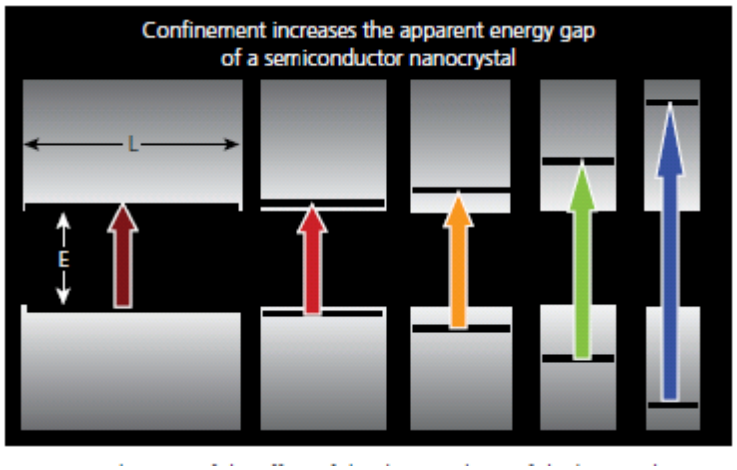

Figure 3.4 Schematic of the effect of the decreased size of the box on the increased energy gap of a semiconductor quantum dot, and the resultant luminescent color change from bulk materials (left) to small nanocrystals (right) [35].

Figure 3.5 shows the type of light emitted as the size of the nanocrystal increases.

Figure 3.5 An example of QDs sorted by size emitting light of different colors excited simultaneously by a single excitation wavelength [36].

It was also reported that open circuit etching led to an increase in the porosity of the material, which was interpreted as a reduction in Si particle size. For these types of samples, near IR and visible intense luminescence (800nm to 700nm) was noted, blue shifting toward orange with increased pore widening treatments. This type of pore widening resulted in some samples having particle size as small as 3nm [34].

Though several experimental and theoretical evidences supporting QCM are discussed in many literatures concerning the model, it is clear that other interpretations are just as valid. One of the most significant problems with the QCM is that no convincing experimental data exist showing a direct relationship between the PL energy and the particle size in P-Si [35].

3.3.2 Surface State Effect

From an optical emitter, the quantum efficiency is defined as the probability of radiative recombination following excitation. The efficiency of Si-ncs, which can decay through radiative decay rate to the total decay rate, as described before QC leads to an enhancement in the radiative rate.

It is generally accepted that the quantum confinement effect in the nanocrystallites opens up the band gap as well as relaxes the selection rules for radiative transitions, giving rise to above band gap PL in the visible region for crystallite sizes below 5nm. However, QCE alone cannot explain the role of various surface treatments and surrounding media. The participation of localized surface states or defects in the oxide has been suggested to influence the PL peak energy and line shape. Interestingly the presence of even a single hydrogen atom is shown to totally distort the small silicon clusters. Since surface to volume ratio increase as the crystallite size decreases, the influence of surface states on the PL from smaller crystallites will be highly enhanced. Furthermore, the role of surface states, especially for low crystallite size, has been clearly demonstrated and explicitly included in PL model.

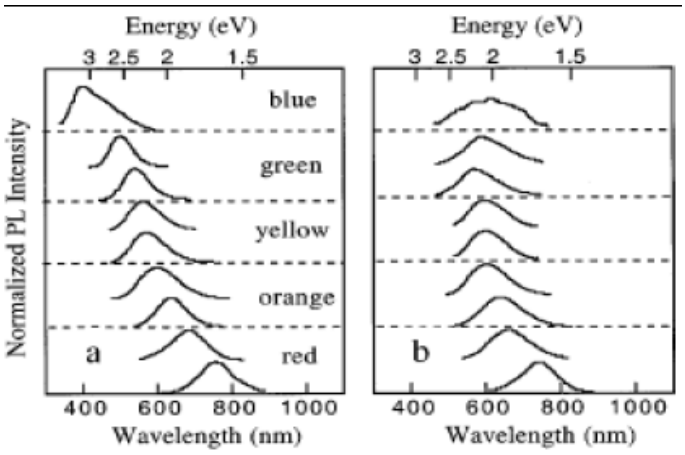

Figure 3.6.Room temperature PL spectra from P-Si samples with deferent porosities kept under Ar atmosphere (a) and after exposure to air (b).

3.3.3 The Quantum Confinement Luminescence Center Model

The quantum confinement model of porous Si which assumes that both the optical excitation and recombination take place inside the nanoscale Silicon particle (NSP), and the energy gap of the particle is enlarged due to the quantum confinement effect, can explain the emission photon energy of PL in the range of visible light. Based on this model a new model, QCLCM was suggested by Qin and Jia in 1996. The main point of view of this model is that the quantum confinement carrier does take place in the NSP, which causes the optical excitation in an energy rage to be much higher than that of the bulk Si band gap and the photo excitation photoemission process can occur outside the NSP.

Chapter Four

Formulation of the Surface State Model

In chapter three we have seen models which describe the PL mechanisms. In this chapter we will formulate the Surface State Model and give quantitative expression for the model considering different parameters which influence the PL mechanism.

4.1. Introduction

We will mix the QC and surface state together. The deriving force for this is that the QCM equation (3.4) alone does not completely explain the observed enhanced PL spectra and energy upshift. Because of the value of C and α are surface, shape, porosity, geometry, size and nature of materials and hence they are highly affected by the environment around so it is important to consider the surface state model together with the quantum confinement model. According to the equation;

$E = \frac{h^2}{8m_oL^2}\left(n_x + n_y + n_z\right)$ n is equal in all direction for quantum dot, hence

$E = \frac{3n^2h^2}{8m_oL^2}$, where $\frac{3n^2h^2}{8m_o}$ is equal to C and m_o is the reduced mass of an electron and a hole which is given by $\frac{1}{m_o} = \frac{1}{m_e} + \frac{1}{m_h}$, m_e and m_h are mass of electron and hole respectively. Substituting the values of the Planck's constant, mass of electron and mass of proton for the hole one can get the value of C approximately 7. And the value of α can be calculated by taking values of Eg from experimental plots of PL versus photon energy graphs (18,37). Note that, the theoretically expected value for α is 2. But experiment shows the value in the range of 1.3- 1.98 depending on the surrounding medium and the value of C is in the range of 3.71-4.55. The deviation of the experimental value from the theoretical is due to the different factors such as shape of the nanocrystalline, geometry, porosity, and type of surface passivation. We believe that the observed PL spectra and band gap upshift is not fully explained by the quantum confinement model alone, hence one should also consider the surface state model to describe the PL spectra and band gap upshift of the nanocrystalline silicon. This is the deriving force for to mix the two models together.

In order to formulate and describe the PL spectra from nc-Si structures, we consider nc-Si as an ensemble of nanometer sized spherical particles having a well

defined size distribution. The optical band gap widening in crystallites is considered due to QCE in nano particles. The magnitude of band gap widening is determined using the analytical expression for band gap obtained from equation 3.4 of section 3.1 in chapter 3. Fig. 4.1 shows various electronic transitions during PL emission from nanocrystallites. On excitation with high energy photons, photocarriers are generated inside the crystallites (path a) and then a fraction of these photoexited carriers relax non-radiatively to the surface states (path c). Subsequently, the relaxed carriers recombine to ground states radiatively giving PL (path d). Since the oscillator strength for direct transition between the LUMO and HOMO (path b) is smaller than that via surface states, we neglect the contributions due to direct transition. The oscillator strength in crystallites is taken to depend on the crystallite size as the inverse power law.

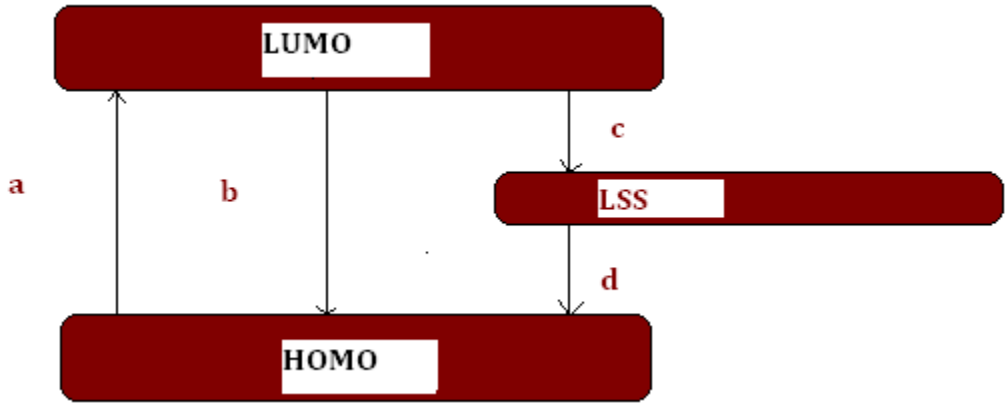

Figure 4.1.Schematic of possible excitonic paths: a) Excitation: ground states (HOMO) to excited states (LUMO); b) De-excitation: LUMO to HOMO band recombination; c) Relaxation: excited states to localized surface states (LSS); and d) Radiative recombination: from LSS to ground state.

Under the above assumptions, the intensity of PL at particular photon energy becomes proportional to the population of occupied surface states and the oscillator strength. The

number of surface states in a crystallite is proportional to the number of atoms on the surface and hence, surface area A of the crystallite. If N_s is the total number of surface states, then

$$N_s \propto A \text{ ----------4.1}$$

Further, if we assume that each atom in a crystallite contributes at least one photoexited carrier to the crystallite, the number of photoexited carriers N_v in a crystallite is proportional to its volume V

$$N_v \propto V \text{----------4.2}$$

The photoexcited carriers inside a nanocrystal relax to the surface states and the recombine radiatively to the ground state. Since the rate of transition from an excited carrier to the localized surface states is proportional to the product of the number of excited photocarriers and the number of available empty surface states in steady state condition, the population N_r of photocarriers in surface states participating in PL processes becomes proportional to the product of above two. That is,

$$N_r \propto VA \text{----------4.3}$$

For a spherical crystallite of diameter L we have $V = \frac{4}{3}\pi L^3$ implies $V \sim L^3$ and $A = 4\pi L^2$ implies $A \sim L^2$. So one gets

$$N_r \propto L^5 \text{----------4.4}$$

The rate of radiative transition depends on the oscillator strength f. The oscillator strength in nanocrystalline materials varies as inverse power law and can be approximated as $f \sim {}^{1}/_{L^{\beta}}$, where power exponent α depends on the material properties as well as the range of crystallites sizes being used. Taking the oscillator strength in to account, the radiative transition probability in a nanocrystallites of diameter L becomes

$$P(L) \propto N_r f \propto L^{5-\beta} \text{----------4.5}$$

Now, the PL intensity from an ensemble of crystallite having size distribution $\varphi(L)$ will be obtained by summing the contributions from all the crystallites having size L. The PL intensity from crystallites of size L may be given by

$$I(L) \propto P(L)\varphi(L) \text{----------4.6}$$

The emitted photon energy from a nanocrystallite will be lower than the band gap energy of the crystallite by an amount of the localization energy E_s of the surface states and the

exciton binding energy E_b. Both, in general, are functions of crystallites size. The emitted photon energy from crystallites will then be given as

$$E_{pl} = E_g + \Delta E - E_s - E_b \text{----------4.7}$$

Where ΔE is the amount of band gap upshift due to QCE in the nanocrystallites and E_g is the band gap corresponding to the bulk crystalline material or

$$\Delta E = E_{pl} - \left(E_g - E_s - E_b\right) \text{----------4.8}$$

According to QCE in the nanocrystallite of diameter L, band gap up shift can be modeled as $\Delta E = {}^{C}/_{L^{\alpha}}$, where C and n are constants due to QCE; their magnitudes strongly depend up on the band gap calculation method being employed. One can transform Eq. (4.6) from L to ΔE dependence by a standard procedure (Fourier Transform).

$$I(\Delta E) \propto \int I(L)\delta\left(\Delta E - {}^{C}/_{L^{\alpha}}\right)dL \text{ ----------4.9}$$

$$I(\Delta E) \propto \int L^{5-\beta}\varphi(L)\delta\left(\Delta E - {}^{C}/_{L^{\alpha}}\right)dL \text{----------4.10}$$

If we take a normal distribution of crystallite sizes in nc-Si, then

$$\varphi(L) = \frac{1}{\sigma\sqrt{2\pi}} exp\left[-\frac{(L-L_o)^2}{2\sigma^2}\right] \text{----------4.11}$$

Where L_0 and σ are the mean crystallite size and standard deviation, respectively, for the nanocrystalline ensemble. Putting Eq. (4.11) in to Eq. (4.10), we obtain the PL expression as

$$I(\Delta E) \propto \int \frac{L^{5-\beta}}{\sigma\sqrt{2\pi}} exp\left[-\frac{(L-L_o)^2}{2\sigma^2}\right]\delta\left(\Delta E - {}^{C}/_{L^{\alpha}}\right)dL \text{----------4.12}$$

$$I(\Delta E) \propto \frac{1}{\sigma}\int L^{5-\beta} exp\left[-\frac{(L-L_o)^2}{2\sigma^2}\right]\delta\left(\Delta E - {}^{C}/_{L^{\alpha}}\right)dL \text{----------4.13}$$

$$L = \left(\frac{C}{L^{\alpha}}\right) \Rightarrow dL = -\frac{1}{C\alpha}\left(\frac{C}{\Delta E}\right)^{\frac{\alpha+1}{\alpha}} d\Delta E \ \ then,$$

$$I(\Delta E) \propto \frac{1}{C\sigma\alpha}\int \left(\frac{C}{\Delta E}\right)^{5-\beta} exp\left[-\frac{(L-L_o)^2}{2\sigma^2}\right]\delta\left(\Delta E - {}^{C}/_{L^{n}}\right)\left(\frac{C}{\Delta E}\right)^{\frac{\alpha+1}{\alpha}} d\Delta E \text{----------4.14}$$

$$I(\Delta E) \propto \frac{1}{C\sigma\alpha}\int \left(\frac{C}{\Delta E}\right)^{\frac{6-\beta+\alpha}{\alpha}} exp\left[-\frac{(L-L_o)^2}{2\sigma^2}\right]\delta\left(\Delta E - {}^{C}/_{L^{\alpha}}\right)\left(\frac{C}{\Delta E}\right)^{\frac{\alpha+1}{\alpha}} d\Delta E \text{----------4.15}$$

Using the properties of Dirac's delta function

$$I(\Delta E) \propto \frac{1}{C\sigma\alpha}\left(\frac{C}{\Delta E}\right)^{\frac{6-\beta+\alpha}{\alpha}} exp\left[-\frac{\left(\left(\frac{C}{\Delta E}\right)^{\frac{1}{\alpha}} - L_o\right)^2}{2\sigma^2}\right] \text{----------4.16}$$

However, it is not uncommon to obtain a log-normal distribution of particle size given by [33]

$$\varphi(L) = \frac{1}{\sigma\sqrt{2\pi}L} exp\left[-\frac{\left(ln(L)-ln(L_o)\right)^2}{2\sigma^2}\right]$$ ----------4.17

This can be used in our approach without loss of generality. With a log-normal distribution the expression for photoluminescence (PL) intensity transforms to

$$I(\Delta E) \propto \frac{1}{C\sigma\alpha}\left(\frac{C}{\Delta E}\right)^{\frac{6-\beta+\alpha}{\alpha}} exp\left[-\frac{\left(ln\left(\frac{C}{\Delta E}\right)^{\frac{1}{\alpha}}-ln(L_o)\right)^2}{2\sigma^2}\right]$$ ----------4.18

Eq. (4.16) and (4.18) give general expression for PL intensity profile from a nc-Si ensemble. It is clear from the above expression that the PL profile will depend strongly on the QC parameters *C* and *α*. Therefore, utmost care should be taken in using the correct QC model for band gap up shift estimation. The oscillator strength and the exciton binding energy E_b both are complicated functions of the size of nano crystallites and their surrounding media. Following careful calculations of *Proot et al* [16] for crystalline silicon, we take α =1.39 and *C*=3.73eV (when L_o is in units of nm) for pure nc-Si. We take a constant value 0.07eV for E_b, which is a fairly good average value for the range of crystalline sizes from ~ 2.5nm to 5nm. The localization energy E_s is taken to be the order of phonon energies which is about 0.05eV for optical phonons. We take E_g as 1.12eV for crystalline silicon at room temperature. Hence, the PL from the silicon nanostructure is a complex process as will be discussed in the next chapter. The main aim here is to compare the experimental observation on photoluminescence intensity variation with our model calculation. In our model we vary crystallite size photon energy which is calculated using equation (3.4) in chapter three, distribution size and the constant values of C and α. Then we take tight-binding and pseudopotential approximation data of crystal size L and the corresponding band gap energy (E_g) and try to fit with our calculation. This is the scope of the next chapter.

Chapter Five

Results and Discussions

5.1 Results

In this chapter, we represent the main results that are obtained based on our model calculation in chapter four and the formula suggested by Ghoshal and et al in chapter three. We also discuss the effect of surface passivation with oxygen and hydrogen on the band gap and PL spectra from silicon nanostructure. In order to obtain the insight in to the effects of the various parameters influencing the band gap and the photoluminescence spectra profile in nc-Si, we computed the band gap and the photoluminescence spectra using relevant fitting parameters in equations (3.4) and (4.16) respectively. The following table show the values of the different parameters used for computation.

TABLE 1: Characteristic parameters used

Sample type	C	α	E_s (eV)	E_b(eV)	Eg^{bulk}(eV)
Pure nc-Si	3.73	1.39	0.05	0.07	1.12
Hydrogen passivated nc-Si	3.82	1.35			
Oxygen passivated nc-Si	3.98	1.33			

Using the above parameters we plot the band gap versus size for different nanocrystalline silicon in a different environment and compare our results with experimental data obtained from the indicated reference by fitting.

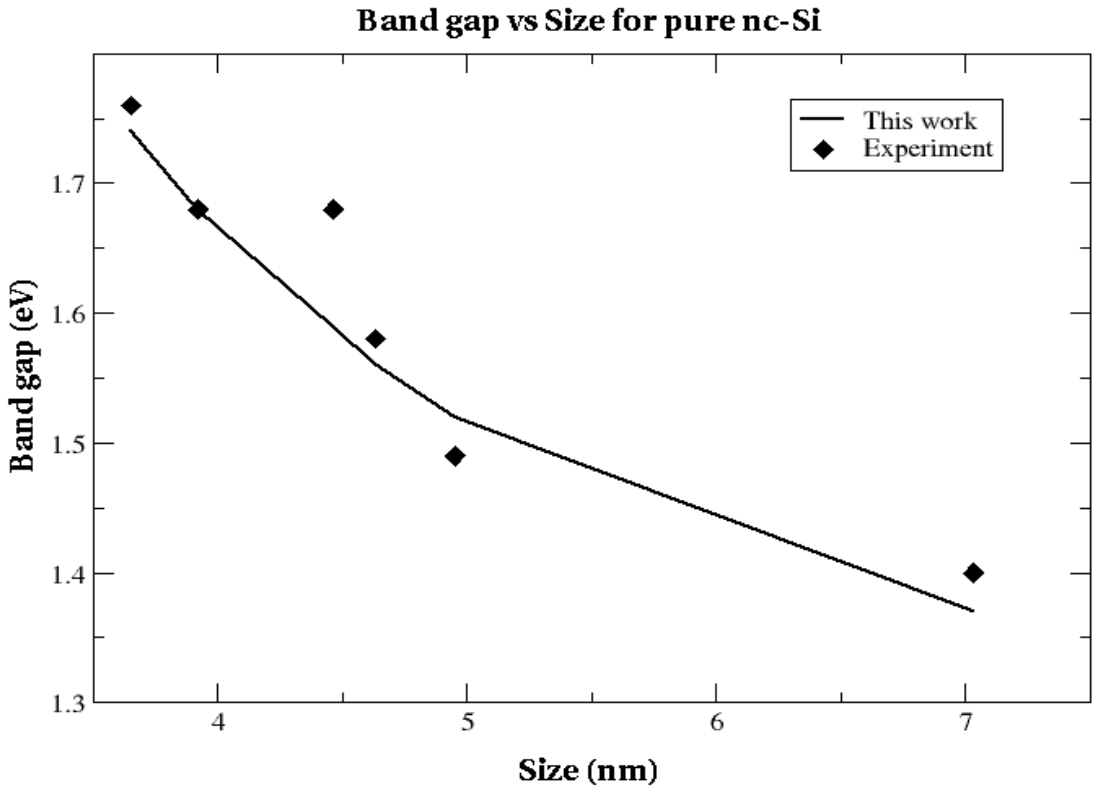

Figure 5.1 Band gap versus size of a pure nanocrystalline silicon (exp from [41])

As it is observed from the graph the band gap of the nanocrystalline silicon increases as the size (diameter) of the quantum dot decreases this implies that the optical properties of the nanocrystalline silicon will change or modified as the size is smaller and smaller. Our work is in a good agreement with the experimental one.

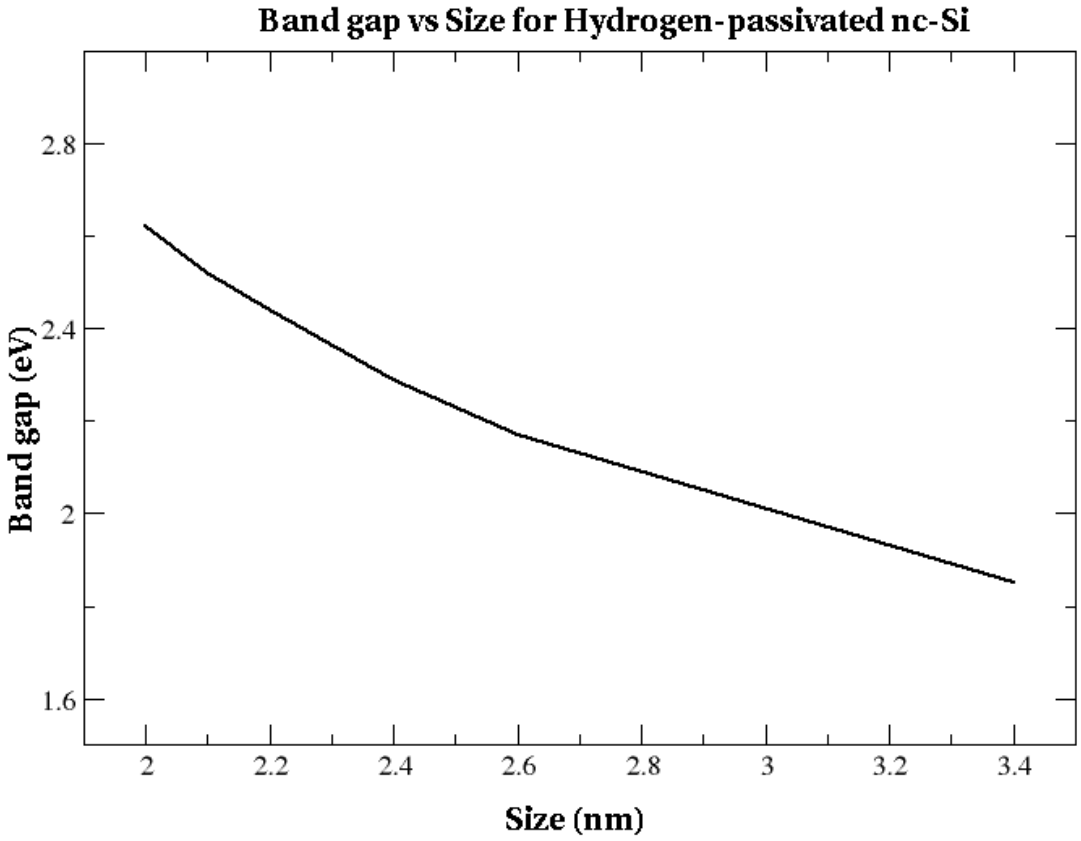

Figure 5.2 band gap versus size of the hydrogen passivated nanocrystalline silicon

We see from the figure, the band gap from the hydrogen passivated silicon nanostructure is higher in energy as compared to that of the pure nanocrystalline silicon quantum dot. This implies that the optical properties of the hydrogen passivated silicon naonostructure will also be modified more. That means the surface passivation has a prominent role in modifying the optical properties of the nanocrystalline silicon.

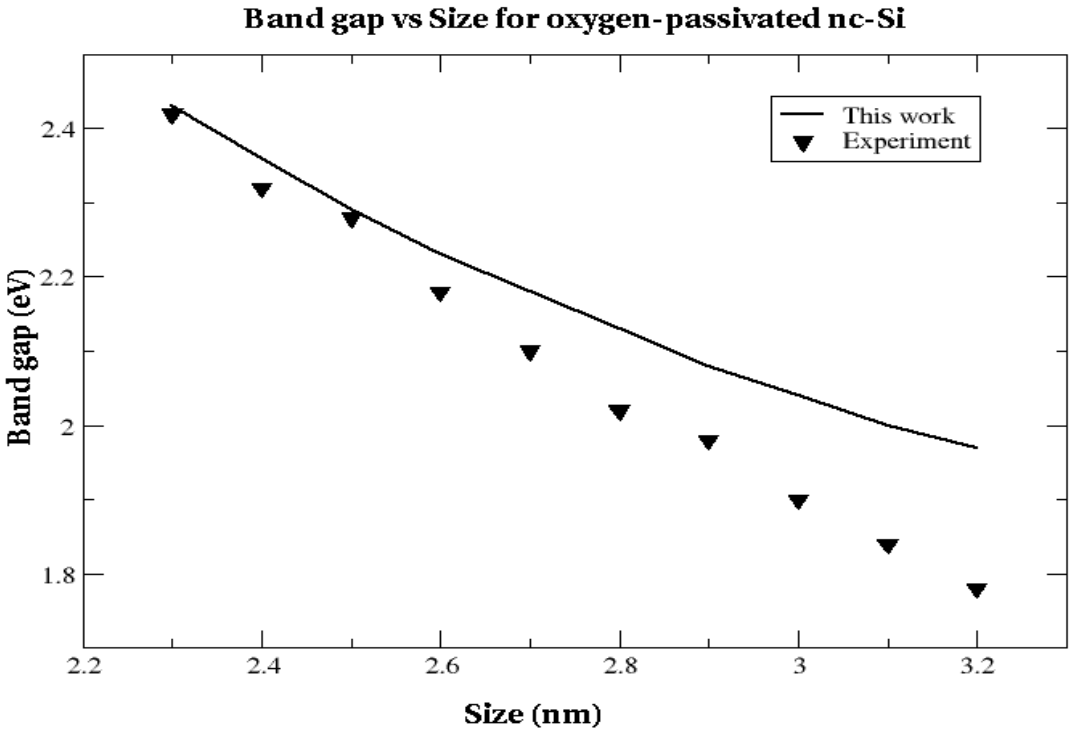

Figure 5.3 Band gap versus size for oxygen passivated nanocrystalline silicon(experiment from 42)

Here again we see the shift in band gap energy of the silicon nanostructure even more than that of the band gap energy shift of the hydrogen passivated nanocrystalline silicon. So we can conclude that the band gap energy increases as the size of the nanocrystalline silicon is diminished and the surface passivation has also great contribution in increasing the band gap energy of the nanocrystalline silicon. The following figure shows the band gap energy of the pure and passivated nanocrystalline silicon drawn all together which will help in comparing the shift in band gap energy for different passivation. Our work has similar trend with the experimental one.

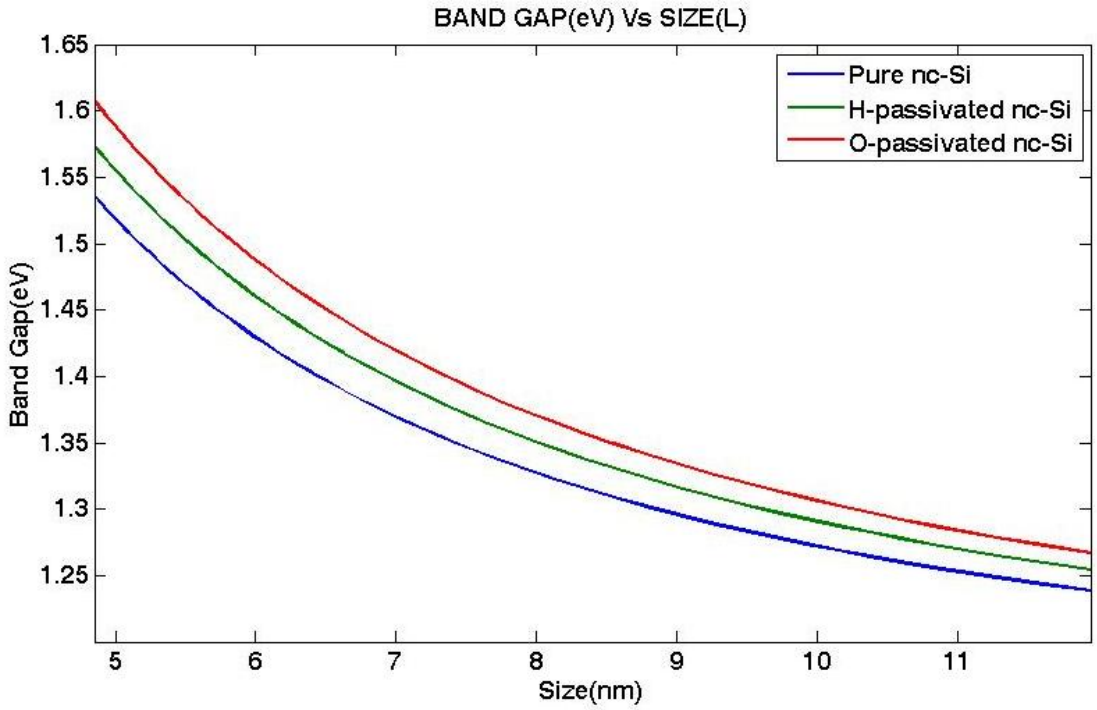

Figure 5.4 the band gap energy versus size of the nanocrystalline silicon for pure, hydrogen-passivated and oxygen-passivated (data taken from [39])

Now let's come on the photoluminescence of the silicon nanostructure. The PL spectra were simulated using equation (4.16) with the typical values of $\sigma \; and \; L_o$ found in the light emitting PS and nc-Si samples. The calculated PL spectra for fixed Lo = 3.2 nm and variable values of σ from 0.16 nm to 0.54 nm are shown in the figure 5.5. As σ increases, the PL spectrum broadens as well as shifts towards low emission energies accompanied by a decrease in relative PL intensity. This implies that the amount of size dispersion affects both the PL peak energy and width.

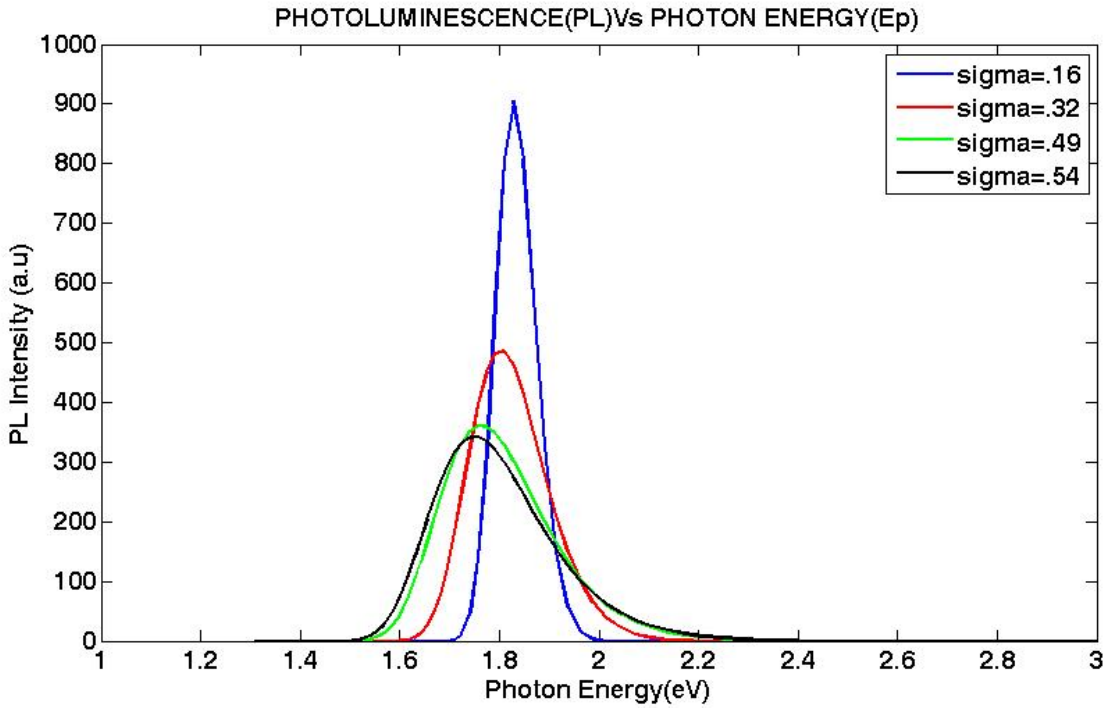

Figure 5.5 PL spectra computed for silicon nanocrystallite having normal crystal size distribution around average mean crystallite diameter, Lo = 3.2 nm at different standard deviation σ

Mean crystallite size Lo being the dominant parameter governing the quantum confinement effect (QCE), the effect of Lo on the PL peak energy is strong. In figure 5.6, calculated PL spectra are shown for three different values of Lo with fixed σ (10% of Lo). Our model depicts the red-shift of PL peak position with increasing mean crystallite size for fixed dispersion.

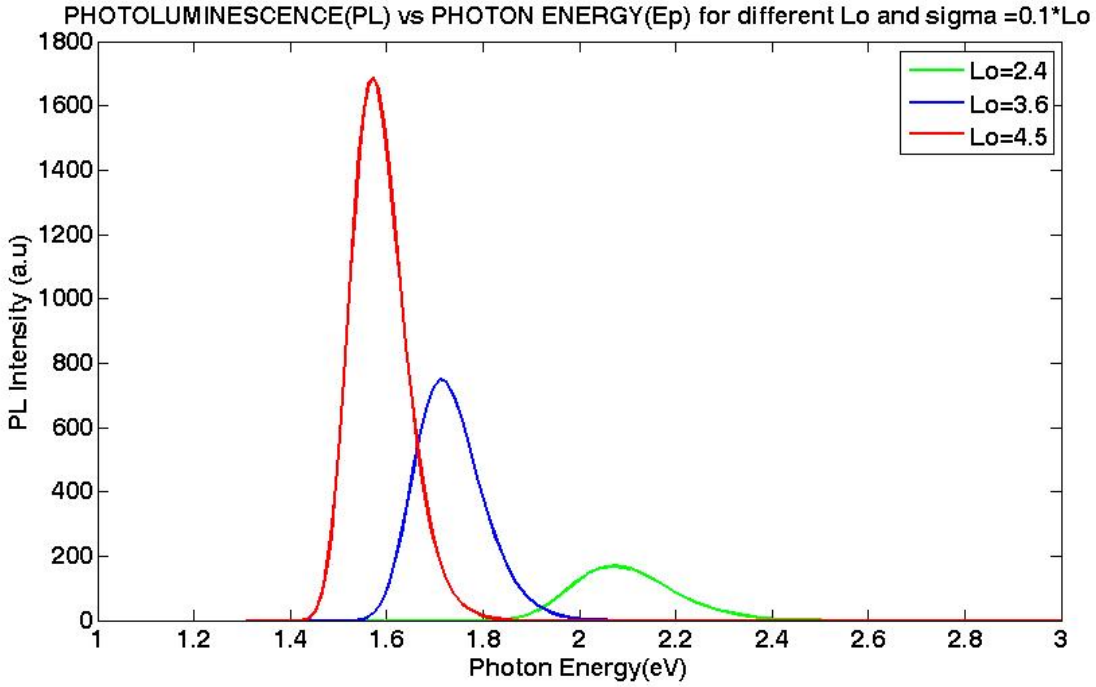

Figure 5.6 PL spectra computed for Si nanocrystallites having normal crystallite size distribution with different mean crystallite diameter Lo and fixed standard deviation $\boldsymbol{\sigma = 10\% \, of \, L_o}$

Different experiments have performed on silicon nanocrystals to see the effect of quantum confinement and surface states. The following figures (5.7-5.11) show the photoluminescence spectra of different samples studied with their size distributions as measured by time-of-flight mass spectroscopy (TOFMS) together with results of our model i.e. normalized photoluminescence intensity versus dots size, for experimental and results of our model for two sets of sample

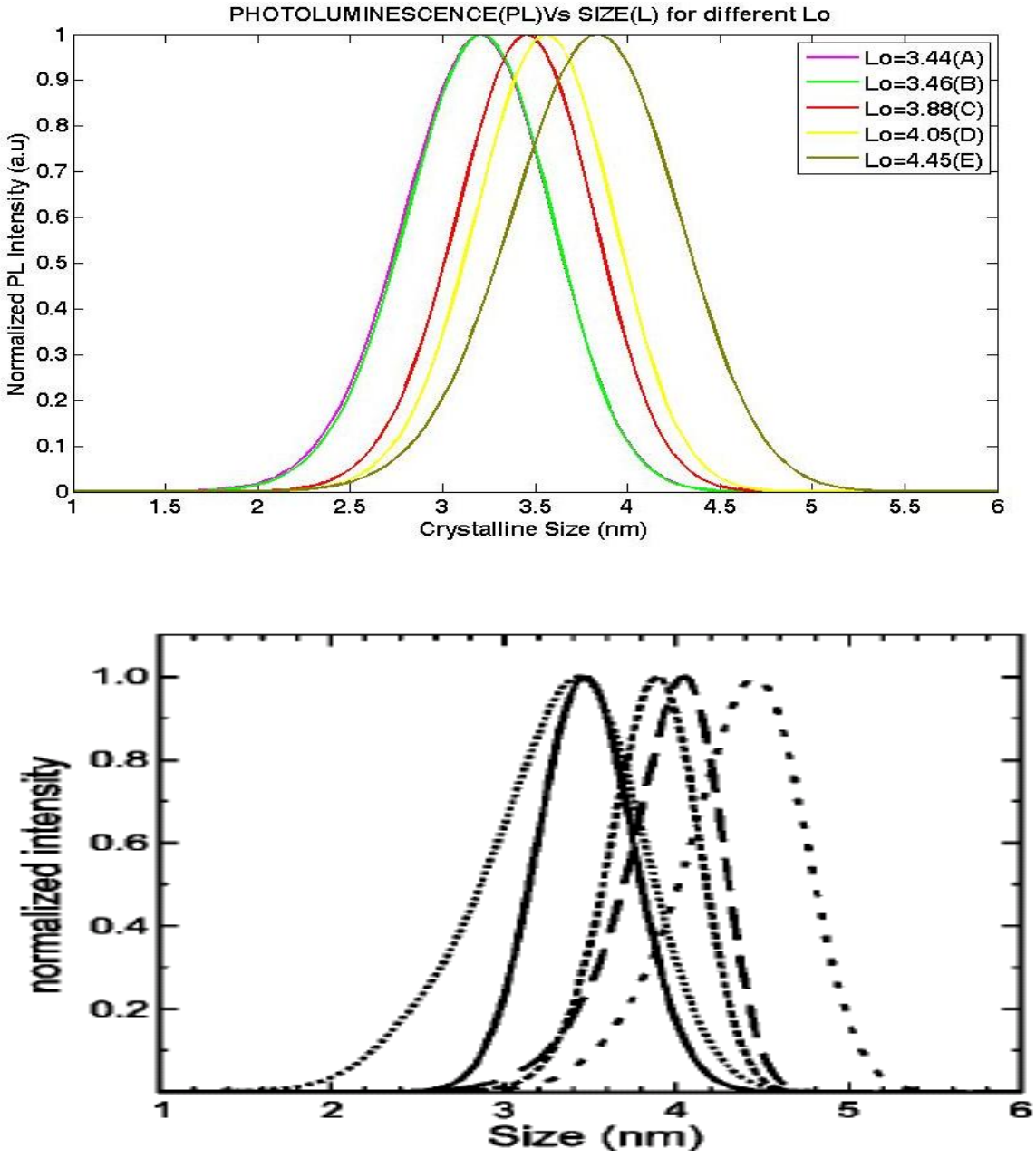

Figure 5.7: Normalized PL intensity versus dot size for the first set of samples Results of our model (upper) Experimental (lower) [37]

When we observe these figures closely, we understood that the photoluminescence peak shifts towards the left that is to the smaller wave length of the visible spectrum (blue shifted) when the average size of nanoparticles becomes small, which is expected. Researchers' realized that width of size distribution and the average size of quantum dots are realities that cause such shifts. For the second set of data we see the same properties as shown below.

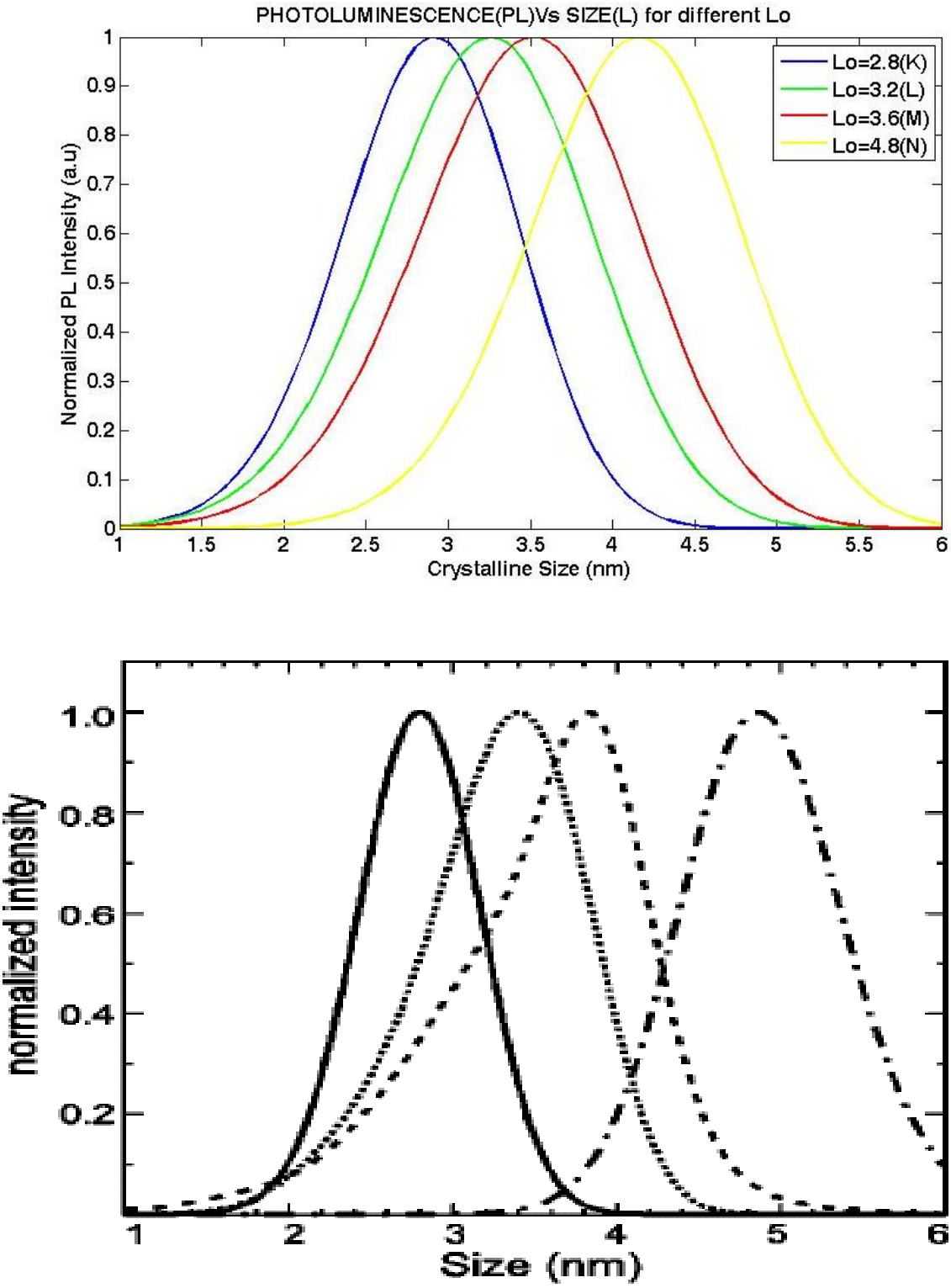

Figure 5.8: Normalized PL intensity versus size for second set of samples Results of our model(upper) Experimental (lower)[37].

For the sake of comparison we report the results of our model and the experimental values taken from G. Ledoux et al [37] are given below in table 5 and 6.

TABLE 2: Characteristic parameters and PL properties of the different nc-Si samples studied [37]

Sample Identifier	Average Size(nm)	Width of Size distribution(nm)	PL Max. (eV)	PL Max. (nm)	PL Width(nm)
A	3.44	1.02	1.82	680	190
B	3.46	0.63	2.03	610	165
C	3.88	0.61	1.75	710	155
D	4.05	0.62	1.65	750	150
E	4.45	0.78	1.55	800	145
K	2.8	0.86	1.95	635	115
L	3.2	1.08	1.71	725	145
M	3.6	1.16	~1.44[a]	~800[a]	~170[a]
N	4.8	1.16	≤1.35[a]	≥900[a]	~200[a]

[a]Values derived from Gaussian fits to the experimental data.

TABLE 3: Characteristic parameters and PL properties of the different silicon nanocrystal samples studied

Sample Identifier	Average size(nm)	PL Max. (eV) Experimental	PL Max. (eV) Results of our model calculation	PL Max. (nm) Experimental	PL Max. (nm) Results of our model calculation
A	3.44	1.82	1.7405	680	684.5
B	3.46	2.03	1.7405	610	684.5
C	3.88	1.75	1.6670	710	714.5
D	4.05	1.65	1.6410	750	726
E	4.45	1.55	1.5727	800	757.5
K	2.8	1.95	1.8491	635	644.3
L	3.2	1.71	1.7248	725	690.8
M	3.6	1.44	1.6538	860	720.4
N	4.8	1.35	1.5160	900	785.9

Just like the size, the photoluminescence spectra of different samples studied with their size distribution as measured by time-of-flight mass spectroscopy (TOFMS) together with results of our model. From such plots, we see that the as average size of the sample decreases the band gap energy increases so that the PL peak shifts to the shorter wavelength range of the visible spectrum. Since, the luminescence energy is directly proportional to band gap energy and inversely proportional to wavelength. Therefore, as the band gap energy increases the PL energy increases or wavelength decreases mostly to the shortest wavelength of visible spectrum. These are shown in the following figures:

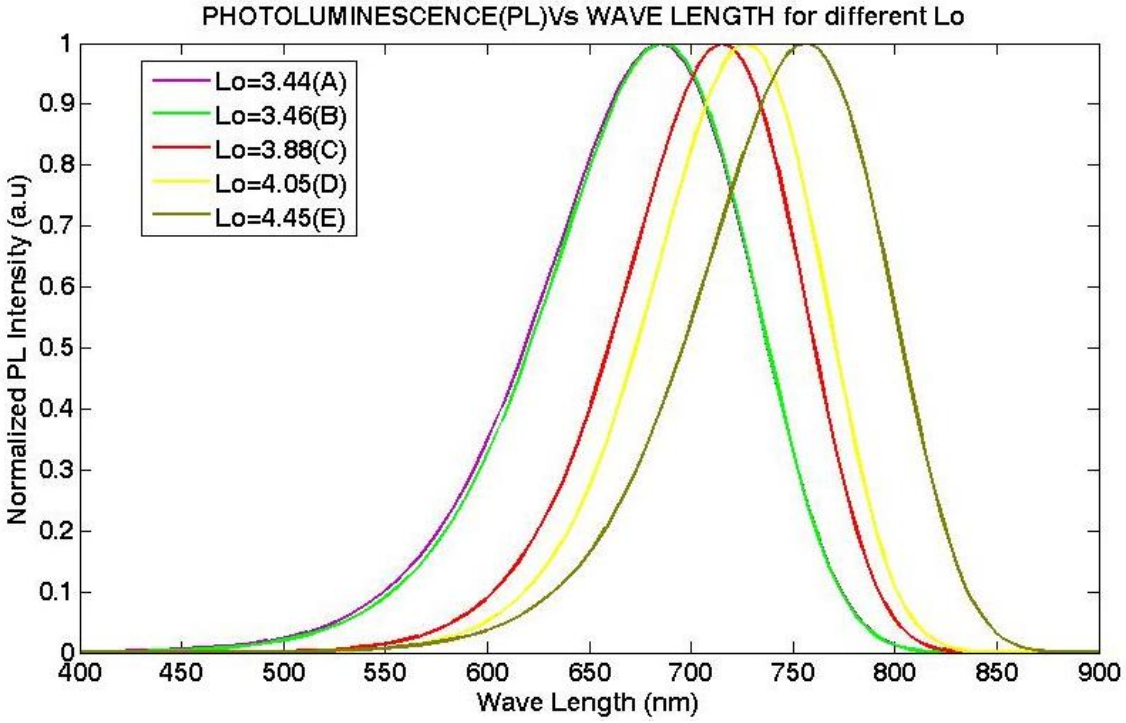

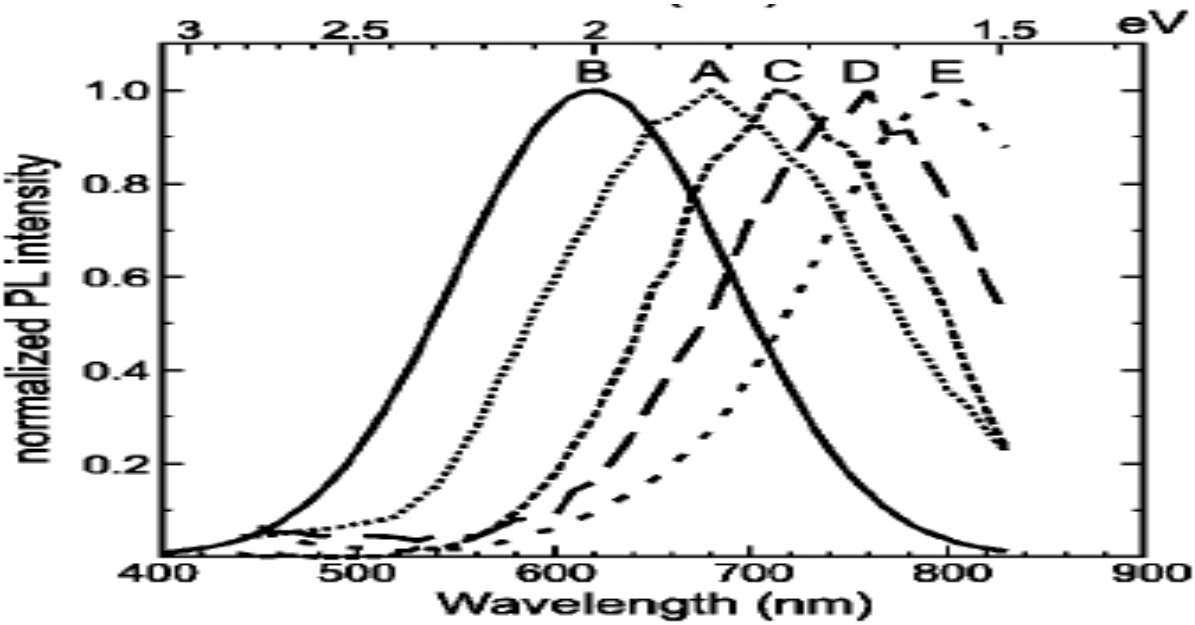

Figure 5.9: Normalized PL spectra versus wavelength for the first set of samples Results of our model(upper) Experimental (lower) [37]

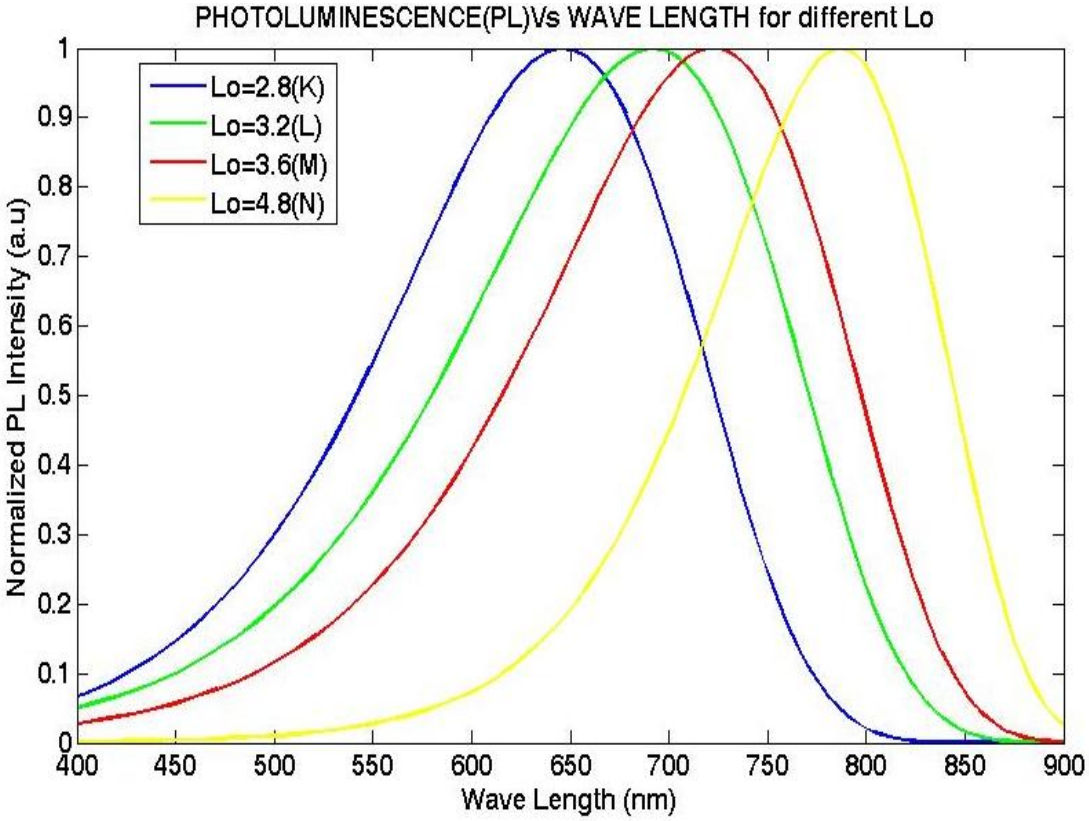

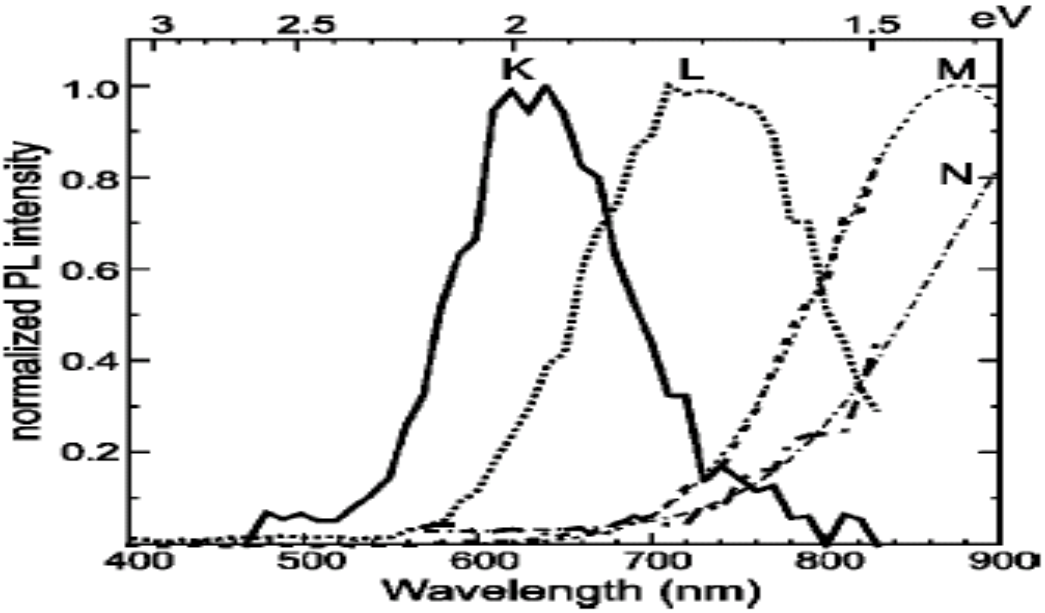

Figure 5.10: Normalized PL spectra Vs wavelength for the second set of samples Results of our model (upper) Experimental (lower) [37]

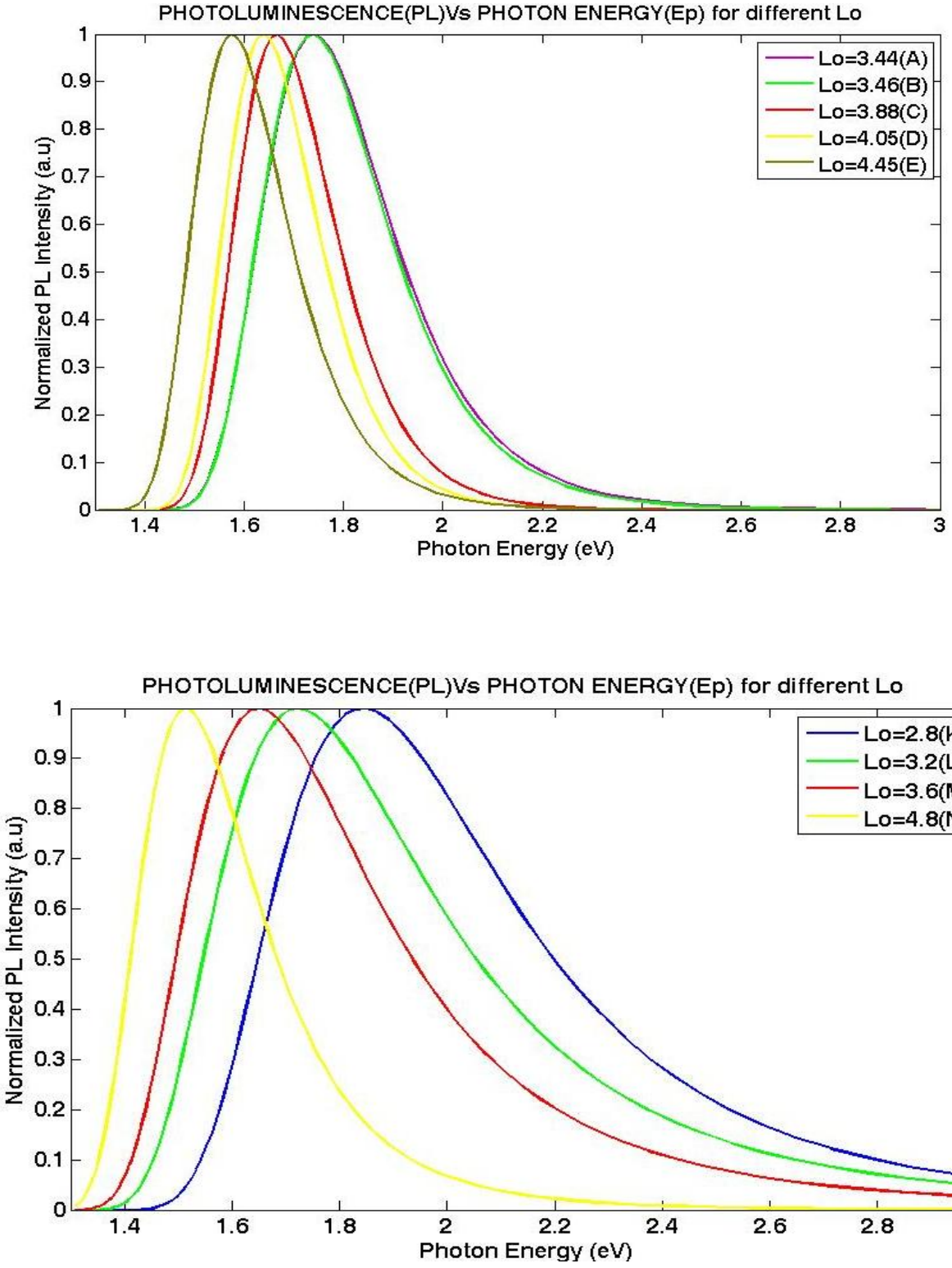

Figure 5.11 Normalized PL spectra Vs photon energy from our model first set of samples (upper) second set of samples (lower)

Note that the experimental graph of PL spectra as a function of photon energy is given in figures 5.9 and 5.10 together with wavelength.

Lastly our model calculation goes on the PL spectra of the pure nc-Si, hydrogen-passivated and oxygen-passivated nc-Si as shown in the figure 5.12, 5.13 and 5.14 respectively. From these figures we see that for fixed value of Lo and σ there is a shift in photon energy of the Si-nanocrystallite size for hydrogen- and oxygen-passivated. This implies that the PL spectra is blue- or red-shifted depending on the surrounding medium around the crystallites

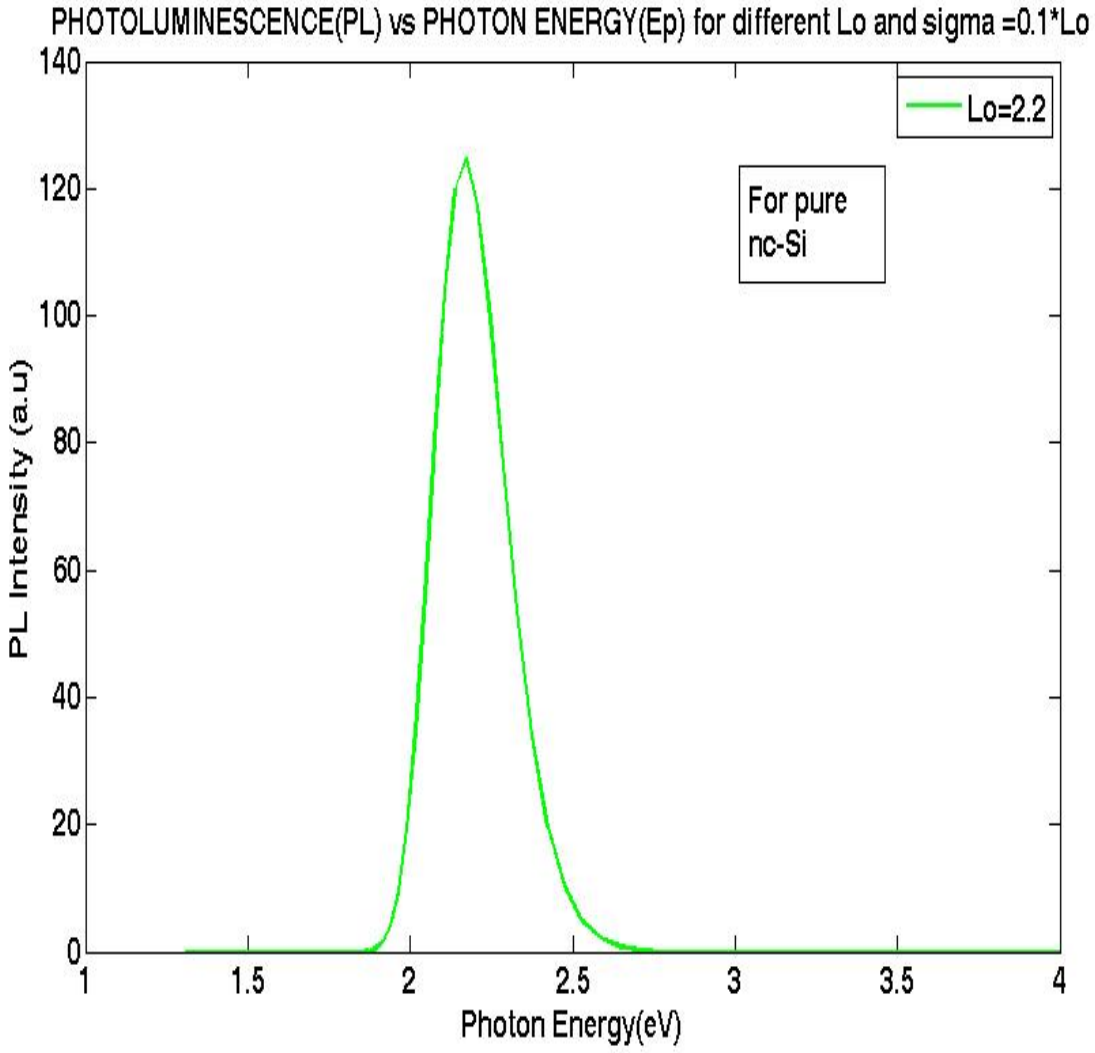

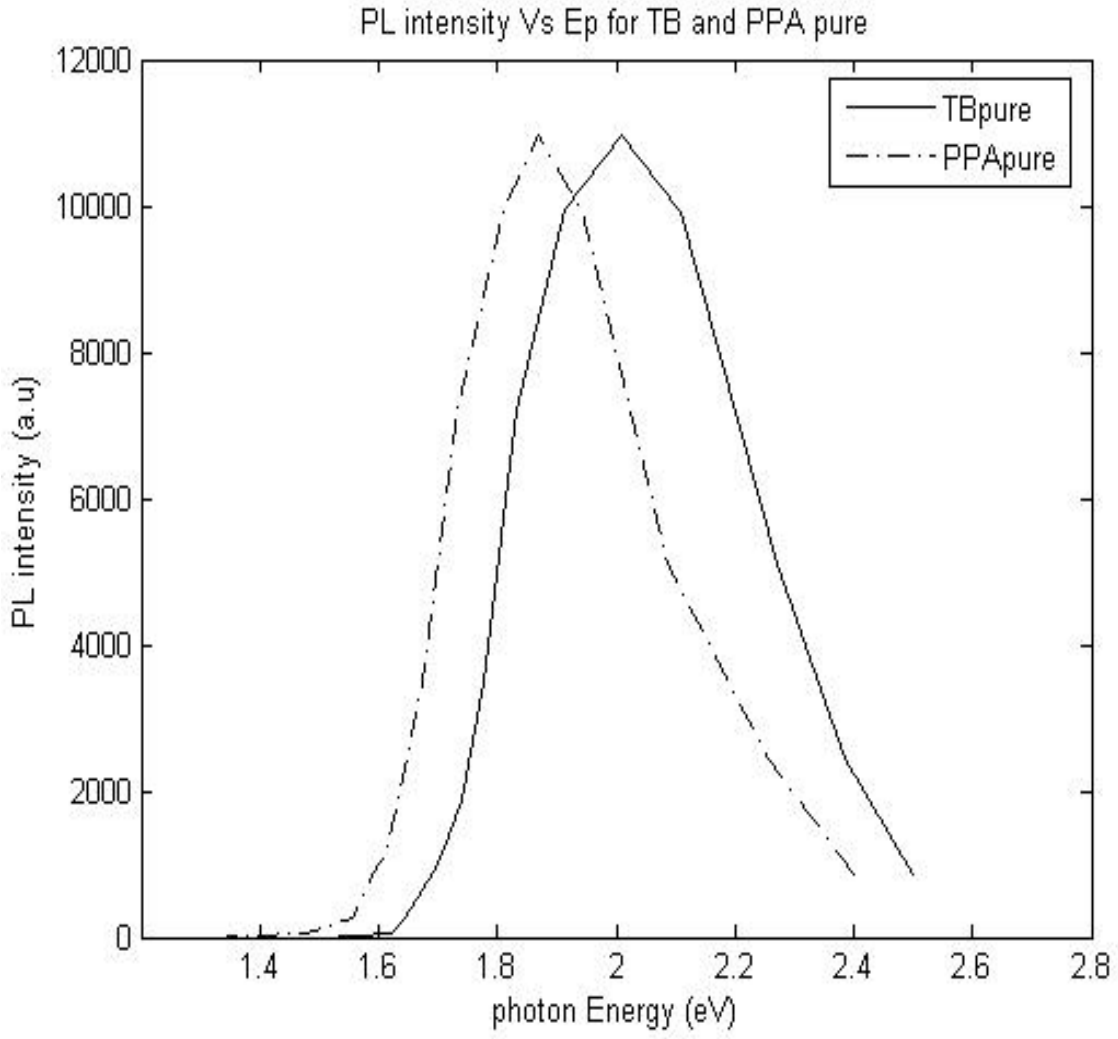

Figure 5.12 PL spectra calculated for fixed mean crystallite diameter, Lo and fixed standard deviation, σ for pure nc-Si having normal size distribution. From our work (upper), TB and PPA schemes (lower).

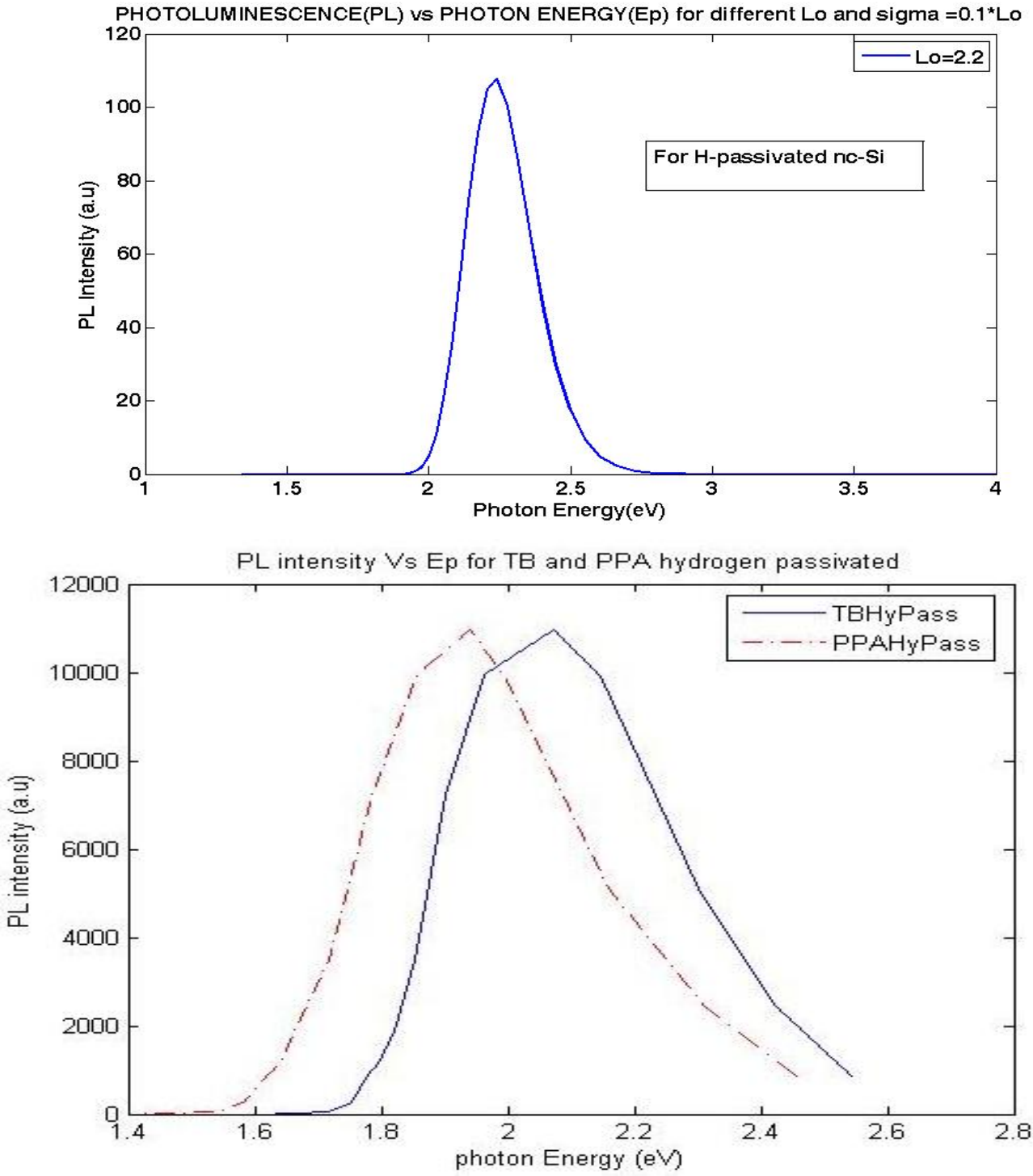

Figure 5.13 PL spectra calculated for fixed mean crystallite diameter, Lo and fixed standard deviation, σ for hydrogen passivated nc-Si having normal size distribution. Our work (upper), from TB and PPA schemes(lower).

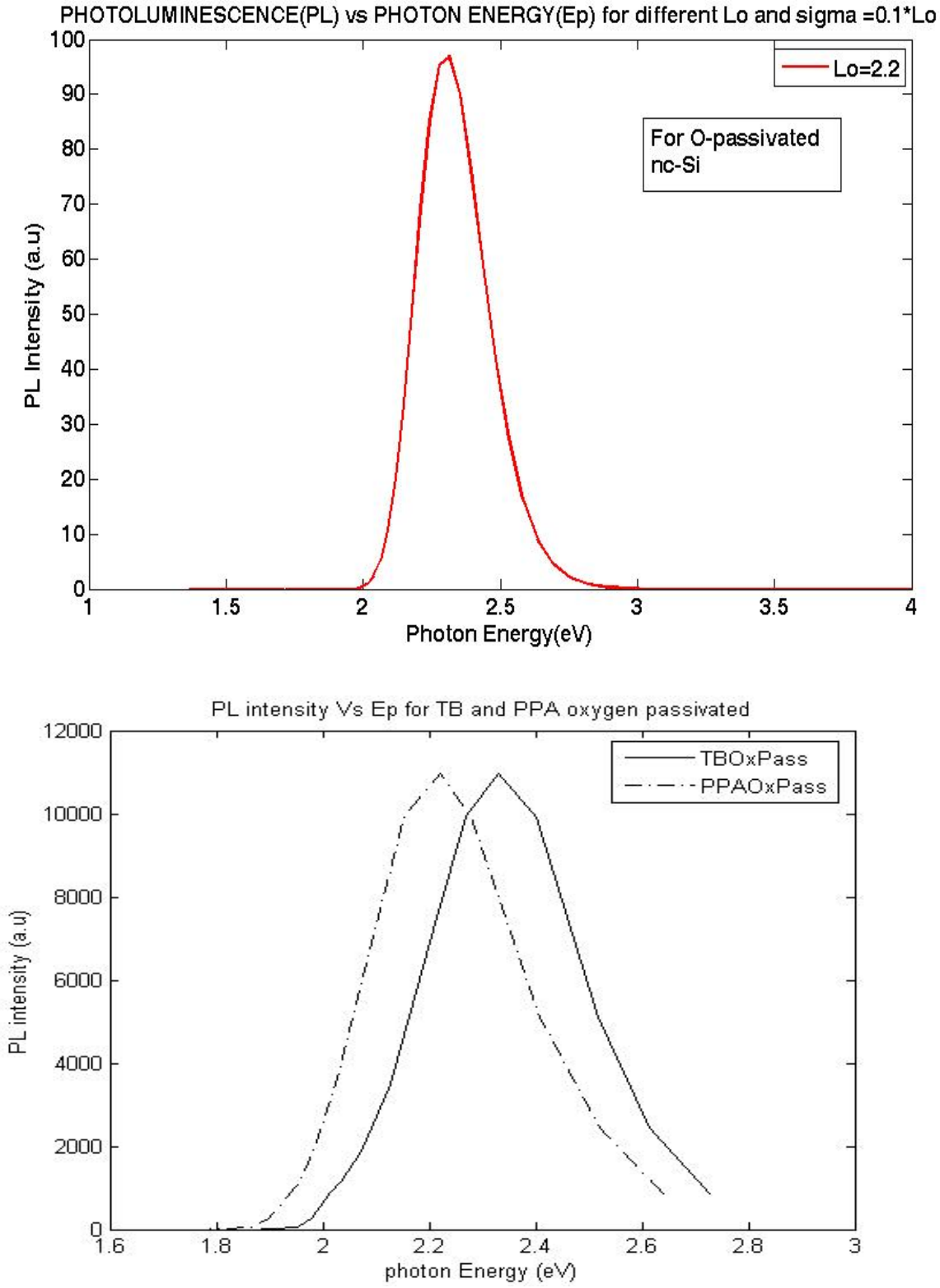

Figure 5.14 PL spectra computed for oxygen-passivated silicon nanocrystallite with fixed mean crystallite diameter, Lo and fixed standard deviation, σ having normal size distribution. Our work (upper), from TB and PPA scheme (lower).

If we carefully observe the photoluminescence spectra of the pure, hydrogen passivated, and oxygen passivated nanocrystalline silicon all are in a good agreement with the other theoretical result. We see some variation in the shift of the photon energy as well as the intensity of the photoluminescence, this may be due to the simplification of our model.

5.2 Discussions

In the variation of the band gap with size of the quantum dot with the experimental may be due to the variation in taking the value of the constants c and α for different environment of the nanocrystalline silicon. As we have mentioned earlier the value of c and α are surface dependant and vary depending on the environment around.

The application of our formulated model requires physical understanding of the parameters used for the system under study in a different environment. A quantitative agreement of the PL model with the experimental PL data depends on the exactness of the average crystallite size and its dispersion, exciton binding energy E_b, and also on the models that estimate band gap and oscillator strength. The exciton binding energy in nanocrystallites is large compared to that in bulk crystals which plays major role. The value of E_b increases monotonically as the crystallite size decreases. While the variation in E_b becomes more pronounced as the crystallite size decreases, it is relatively flat for larger crystallites. According to theoretical calculations [38, 39] E_b varies from 0.05 to 0.12eV for the crystallite size range of 4-2.5nm for crystalline silicon in a different environment. Therefore, the constant value of E_b =0.07eV taken earlier over the mean crystallite size ranging from 2.5 to 4nm introduces negligible error in our PL calculation.

The presence of surrounding media for the crystallites further complicates the analysis of observed PL data. The degree of localization of surface state (manifested by E_s) depends on the amount of disorderness in surface atoms of crystallites. The different surface passivation will give rise to a variable amount of disorder. Therefore, the localization energy E_s will depend on the type of surface passivation. It has been shown that the hydrogen and oxygen termination of surface atoms in PS gives a PL spectrum having a shift of about 0.14 to 0.18eV in PL peak energy for the same crystallite sizes [40].

We believe that our simple minded model could provide a nice qualitative picture of the observed PL. However, for detail nature of the PL spectra much more serious calculations are needed that cover complete descriptions of the nanostructures.

Chapter Six

Summary and conclusion

In this thesis we have presented the variation of the band gap of nanocrystalline silicon as a function of size and the different passivation of the nanocrystalline silicon, for simplicity we have considered the nanocluster of spherical in shape. And we observed that the role of the surface is very crucial like that of the quantum confinement effect on the band gap as well as the photoluminescence as we see below. We have also presented analytical expressions for PL by unifying the quantum confinement effects and localized surface states to describe experimental PL spectra from silicon nanostructures. The role of surface states, especially for low crystallite sizes, has been clearly demonstrated and explicitly included in the PL model. The model is able to predict the published experimental PL data on silicon nanostructures produced by a variety of experimental techniques. Our work shows the importance of surface passivation and effect of crystallites size in predicting the PL data from nanocrystalline silicon using quantum confinement models. The present model is useful in understanding the role of surface passivation and surrounding media on the PL process in nc-Si.

The role of quantum confinement model is to treat nc-Si as the atomic like structure. The model enables us to observe clearly the PL from nc-Si with varying mean crystallite size. The PL spectra from nc-Si can be enhanced by passivating the surface with hydrogen or oxygen. In this thesis we studied the band gap and PL spectra of hydrogen and oxygen passivated nc-Si samples, mainly quantum dots. Our results show that the effect of oxygen terminated surface on the band gap and PL spectra from nc-Si is more pronounced than hydrogenated surface because of stability difference they made on the surface. This is in a good agreement with the experimental value. For a PS sample free from oxidation, the QCM dominates. When the nanosilicon particles (NSPs) is oxidized, PS sample have very small density or large sizes, and photo emission occur in LCs in the Si-oxide layers is dominating. Thus, more than one type of PL mechanism models are important.

We believe that our simple minded model can be further extended to other quantum structures (quantum well and quantum wire) and also to varying porosity. In real sample a set of size distribution is possible with different mean length that may be an interesting thing to look at other mechanism that might affect the PL are: luminescent center, porosity, bond distortion and shape of quantum dots that can be incorporated for more realistic calculation.

We have used the data from tight-binding and pseudo-potential to generate the PL spectra. It is how ever, worth to take the data from DFT luminescent center model and then fit to our model to compare the experimental PL. Our results are in conformity with some of the recent experimental and theoretical observations.

In general, we believe that our surface state model that includes QC and surface passivation is able to explain qualitatively the experimental observation of visible PL from porous as well as nanocrystalline silicon. This study is in conformity with other model calculations and theoretical predictions. It is worth to look at multiple distributions of crystal sizes to get a better estimate of visible PL. The result obtained can be utilized for the control of light emitting properties in device fabrication.

This model can be extended to study optical behaviors like, Oscillator strength, Radiative Recombination Life Time, Absorption Coefficient, Dielectric Constant, and Density of states from nanocrystalline silicon which has tremendous applied interest. We can also study the temperature and pressure dependence of visible PL from nanocrystalline silicon. The light emission from quantum wires and quantum wells can also be examined by modifying the model to shape and size dependence. The role of bond distribution, impurities, phonons, excitons, and relaxational mechanism are some of the open questions that has to be addressed for accurate quantification of visible PL. in case of porous silicon the varying porosity along with crystallites size play role in deciding PL. in our model this is not included. The trap centre and luminescent centre also affects the nature of PL spectra.

References

[1] S.Limaye, S.Subramanian, B.Goller, J.Diener, and D.Kovalev, Phys. Stat. Sol. (a) 204, No**. 5**, 12971301 (2007)

[2] S.Botti, M.L. Terranova, V.Sessa, S.Piccirillo and M.Rossi, Appl. Organometal. Chem, **15,**388392 (2001)

[3] M. Ehbercht, B. Kohn, F. Huisken, M. A. Laguna, V.Paillaid, Phys. Rev. B **56**, 6958 (1997)

[4] C. Delerue, G. Allan, M. Lanno, Phys. Rev.B **48,** 11024 (1993)

[5] Y. Kanemistsu, H. Hutu, Y. Masumota, T. Fulgati, H. Mimura, Phys. Rev. B **48,** 2827 (1993)

[6] Y.Kanetsu, N. Shimizu, T. Komoda, P. Hemment, B. Sealy, Phys. Rev. B **54** , 14329 (1996) and reference cited therein

[7] P. Grantzer and K. Rumpf, Mat.**,3,** 943-998 (2010)

[8] http://w.w.w.ece.nus.edu.59/coe/, Nussni, Focus Groups 2006 Research Abstract (Nanophotonics) visited on 17, March 2010.

[9] B. Podro, Zs. J. Horvath and P. Basa, Semi. Nano. **2,** 411 (2005)

[10] W. C. Choi, C. K. Kim, E. K. Kim, C. M. Shim, D. Jung and C. Y. Park, J. Kor. Phys. Soc. **36**, 23 (2000)

[11] Brian A. Korgel, SPIE Newsroom, **10,** 11172/1200607.0203, **4** (2006)

[12] V. Sivakov, G. Andra, A. Gawlik, A. Berger, J. Plentz, F. Falk and S. H. Christiansen Vol. 9, No. **4,** 1549-1554 (2009)

[13] Daniel Miloni, John Wiley and Sons, Inc. **106** (2006)

[14] Edward L.Wolf, Wiley-VCH, **40** (2004)

[15] L. T. Canham, Appl. Phys. Lette. **57**, 1064 (1990)

[16] J. P. Proot, C. Delerue and G. Allan, App. Lette. **61**, 1948 (1992)

[17] Kenji Imakita, Masahiko Ito, Minoru Fuji and Shiniji Hayashi Vol. 17, No. **9**, /OPTICS EXPRESS 7368 (2009)

[18] M. V. Wolkin, J. Jorne, P. M. Fauchet, G. Allan and C. Delerue, Phys. Rev. Lette.**82,** 197 (1999)

[19] Tae-Youb Kim, Nae-Man Park, Kyung-Hyun Kim, Young-Woo Ok, Tae Yeo Seong, Cheo-Jong Choi and Gun Yong Sung, Mat. Res. Soc. Symp. Proc. Vol. 817, **78** (2004)

[20] J. I. Pankove, Optical Processes in Semiconductors, Prentice-Hall, Englewood Cliffs, New Jersey, 1971.

[21] Karl W. Böer, Survey of Semiconductor Physics: Electrons and Other Particles in Bulk Semiconductors, Nostrand Reinhold, 1990.

[22] P. Bettoti, M. Cazzanelli, L. Dal Negro, B. Danese, Z. Gaburro, C. J. Oton, G. Vijaya, Prakash and L. Pavesi, J. Phys. Cond. Mat. **14**, 8253 (2003).

[23] P. K. Basu, Theory of Optical Processes in Semiconductors: Bulk and Microstructures, Oxford University Press, Oxford, England, 1997.

[24] Sender OGUT, Turk J. Phys. **27**, 443-458 (2003)

[25] Neil W. Ashcroft and N. David Mermin, Solid State Physics, Saunders College (1976)

[26] P. Hohenberg and W. Kohn, Phys. Rev. B **864,** 136 (1964)

[27] W.Kohn and L. J. Sham, Phys. Rev. A **1133**, 140 (1965), M. T. Yin and M. L. Cohn, Phys. Rev. B **25**, 7403 (1982)

[28] A. Zunger and L-W. Wong, Applied Surface science, **102**, 350 (1996)

[39] S.Tripathy, R. K. Soni, S. K. Ghoshal and K. P. Jain, Bull. Mater.Sci. Vol. **24**, 285 (2001)

[30] S. K. Ghoshal, Asian, J. Spect **7,** 49 (2003)

[31] S. K.Ghoshal, Devendera Mohan, Tadesse Tenaw Kassa and Sunita Sharma, Int. J. Mod. Phys., B **21**, No. 22,3783 (2007)

[32] Kanemitsu Y, Suzuki K, Uto H, Masumoto Y, Matsumoto T, Kyoshin S, Higuci K and Matsumoto H, Appl. Phys. Lette., **61** (2446) http://link.aps.org/abstract/PRB/v68/e085309

[33] S. K. Ghoshal, U. Gupta and K. S. Gill, Ind. J. Pure & Appl. Phys. **43**, 188 (2005).

[34] T. VanBurren, L. N. Dinh, L. L. Chase, W. J. Seikhaus, and L. J. Terminello, Phys. Rev. Lett. **80**, 17 (1998).

[35] Mark Asta, Susan M. Kauzlaric, Kailiu, Alexandra Navrotsky, and Frank E. Ostreloh Vol.2, No.1 (2007).

[36] V. Adam, J.Drbohlovova, R. Kzek and J. Hubalek Int. J . Mol. Sci. **10,** 656-673 (2009)

[37] G. Ledoux, O. Guillois, D. Porterat and C. Reynaud, Phys. Rev. B, **62,** 23 (2000)

[38] T. Takagahara and K. Takeda, Phys. Rev. B **46**, 15578 (1992).

[39] M. Lannoo, C. Delerue, and G. Allan, Phys. Rev. Lett. **74**, 3415 (1995).

[40] T. Matsumoto, G. Arasta, S.V. Nair, and Y. Masumoto, Jpn. J. Appl. Phys. part 1 **38**, 589 (1999); T. Matsumoto, Y. Matsumoto, S. Nakashima, and N. Koshida, **297**, 31 (1997).

[41] M. Ehbrecht, B. Kohn, F. Huisken, M. A. Lguna and V. Pillard, Phys. Rev.B, **56** ,11(1997)

[42] J. S. Biteen, N. S. Lewis, H. A. Atwater and A. Polman App. Phys. Lett. **84** ,26(2004)